BMC Biology

METHODOLOGY ARTICLE

Open Access

Sex- and social context-dependent differences in mice fine head movement during social interactions

Adèle Phalip[1*], Shai Netser[1] and Shlomo Wagner[1]

Abstract

Background Social decision-making is influenced by multiple factors such as age, sex, emotional state, and the individual's social environment. While various behavioural readouts have been commonly used to study social behaviour in rodents, the role of fine head movements during social interactions remains underexplored despite the presence of accelerometers in many electrophysiological recording systems.

Results Here, we used head acceleration data to analyse head movement kinematics in adult male and female mice across several social discrimination tests in various time scales. Our findings demonstrate the complementary nature of two variables derived from the raw acceleration, namely overall static (OSHA) and dynamic (ODHA) head acceleration, as well as specific head angles (Pitch and Roll). Together, these variables provide a comprehensive, detailed analysis of head movement, which cannot be easily achieved by video analysis systems such as DeepLabCut. Overall, our results suggest that head movement patterns are significantly influenced by sex, stimulus preference, and social context. Specifically, ODHA exhibited strong sex dependence and appeared to be more sensitive to internal states such as arousal and alertness. The static components were primarily influenced by social context, particularly stimulus preference, and seemed to reflect the subject's motivation to engage with the stimulus. The Roll angle also appeared strongly modulated by the broader social context.

Conclusions Our study provides a novel method and analysis pipeline for studying the social behaviour of small rodents in high-time resolution using a head-based accelerometer. Our findings suggest that such measurements may inform the affective and motivational states of the subject during social interactions.

Keywords Accelerometer, Social behaviour, Head movement, Small rodents, Social discrimination, Affective states

Background

Social behaviour is a fundamental and highly complex type of behaviour which is necessary for survival [1]. Rodents respond to their social environment with flexible and context-appropriate behaviours. The decision to approach or avoid a conspecific requires the integration of perceived social cues with environmental and internal factors such as social rank, age, familiarity and sex [2–4]. Social decision-making is also influenced by the emotional states of others [5, 6]. Accordingly, social behaviour involves several cognitive processes, such as social cues perception, social context assessment, social recognition and internal-state evaluation, which lead to adaptive social decision-making. To study these processes, scientists commonly look at various types of behavioural readouts, such as the time spent interacting with a conspecific, the vocalisations emitted by the individual, or its micturition activity [7].

*Correspondence:
Adèle Phalip
adele.phalip@gmail.com
[1] Sagol Department of Neurobiology, Faculty of Natural Sciences, University of Haifa, Haifa, Israel

In natural conditions, sensory integration generally occurs in the context of ongoing head movements, which thus may serve as a primary behavioural readout of the individual's motivation and intention [8]. Moreover, it has been shown that significant components of the neural activity in sensory cortices during behaviour reflect multiple aspects of movement across species [9–11]. Lastly, locomotion is closely coupled with arousal [12]. These findings suggest a potential link between head movement and the processing of social cues. To address this issue in rodents, one needs to identify quantitative variables that reliably and unbiasedly reflect the head movement of rodents in fine time resolution, which may allow to align them with specific patterns of brain activity.

Accelerometers are used in various fields nowadays, whether to study animals' movement in their environment [13–18], to understand sleep disorders [19], or to assess movement disorders such as Parkinson's [20]. They are also used to detect falls in people at risk [21]. However, in laboratory rodents, this tool has been scarcely utilised. At one point, this was attributed to the device's size, but for several years now, it has been adapted for small animals such as mice or rats. The few studies employing accelerometers in laboratory animals mainly focused on locomotion [22–25] or sleep analyses [26]. Notably, many headstages of electrophysiological recording systems contain an accelerometer chip, which could be a powerful tool for measuring head acceleration in three axes, hence offering a potential means to analyse head movement in various contexts. However, this tool was hardly used to study animal social behaviour in a detailed manner.

Head motion can be characterised by the angle (roll, pitch and yaw) and the speed change in three directions (x, y and z axis). Acceleration results from the force of gravity combined with changes in speed and direction. Thus, it comprises two components: static acceleration, which reflects the accelerometer's inclination relative to Earth's gravity and indicates changes in posture, and dynamic acceleration, which reflects changes in velocity along each axis. Static acceleration measured along three axes enables the calculation of the body's pitch and roll angles (henceforth termed Pitch and Roll, respectively) [17, 27]. Pitch is calculated as the Arcsine of the static acceleration on the y-axis, while Roll is similarly derived from the static acceleration along the z-axis. Yaw, however, is not influenced by gravity and, hence, cannot be calculated directly from the acceleration data.

Wilson et al. (2006) [28] established a method based on the concept that, in most vertebrates, energy expenditure primarily results from movement [29–31]. Accordingly, body acceleration should correlate with energy expenditure [28, 32–34]. Overall Dynamic Body Acceleration (ODBA), the Euclidean norm of the high-pass filtered 3D body acceleration, was thus developed as a comprehensive measure of body motion across three spatial dimensions, showing a significant correlation with energy expenditure [35].

Here, we used the Overall Dynamic Head Acceleration (ODHA) and Overall Static Head Acceleration (OSHA), along with the Roll and Pitch angles, to analyse the head movements of adult male and female ICR (CD-1) mice during various social discrimination tests (social contexts). By analysing these variables across various time windows, we demonstrated that OSHA, Roll and the Pitch provide insight into the posture of the animal's head. At the same time, ODHA serves as an approximation of the energy expended during rapid head movements. By comparing these measurements to video analysis using DeepLabCut, we show that head acceleration-based variables offer precise head kinematic measurements, capturing nuances not discernible through direct observation or video analysis. Finally, our analyses of head acceleration during social investigation unveiled that the ODHA signal is sensitive to alerting events and influenced by sex, while the OSHA signal was more sensitive to stimulus attractiveness.

Overall, our study provides a novel method and analysis pipeline for studying the social behaviour of small rodents in fine time resolution using a head-based accelerometer.

Results

Behavioural dynamics of ICR mice across four distinct binary social discrimination tests

Female ($n=22$) and male ($n=12$) ICR mice were recorded during the four behavioural tests described below, conducted across three days (two sessions in the morning and two sessions in the afternoon), typically in the order shown in Fig. 1A. We used a video camera located above an experimental arena containing two stimulus chambers in opposite corners (Fig. 1B), as previously described [36–38], to record the investigation behaviour of subject mice towards two distinct stimuli in each session. In the social preference (SP) test, subjects encountered a novel sex-matched juvenile conspecific (social stimulus) vs. a Lego toy (object stimulus). Male vs. female age-matched conspecifics were used as stimuli for the sex preference (SxP) test, while stressed vs. non-stressed (naive) sex- and age-matched animals were used as stimuli for the stress-state preference (SSP) test. Finally, isolated (7–14 days) vs. group-housed age- and sex-matched animals were used as stimuli in the isolation-state preference (ISP) test.

The mice were recorded for 15 min: 5 min before the test (pre-test stage), 5 min during the test (test stage), and 5 min after the test (post-test stage). During the

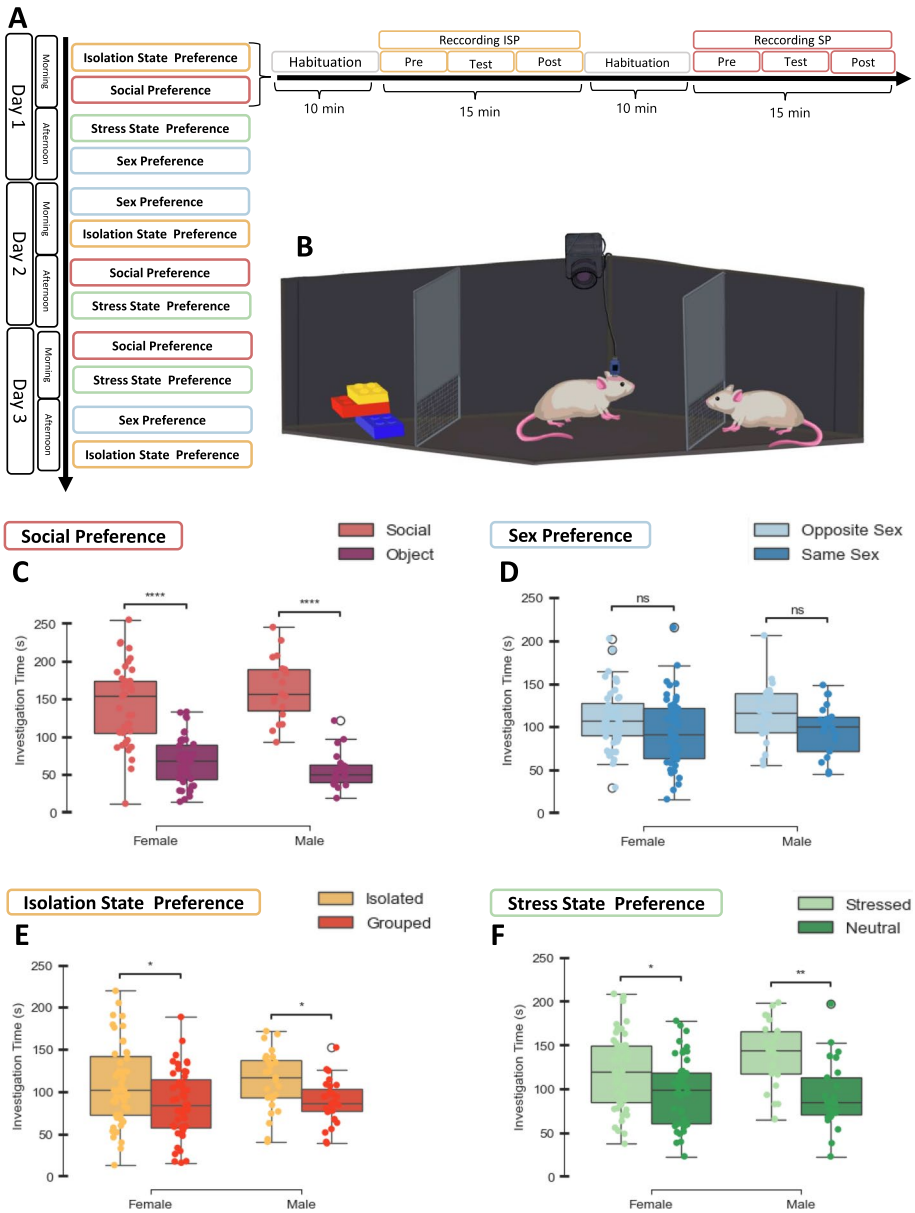

Fig. 1 Stimulus investigation time across four social discrimination tests. A Timeline of the various tasks conducted by the recorded mice. **B** Schematic representation of the set-up. (**C**) Mean investigation time was measured separately for each stimulus during the social preference (SP) test for males ($t = 7.50$, $p < 0.001$) and females ($t = 6.53$, $p < 0.001$) mice. **D** As in (**A**) for the sex preference (SxP) test (*Males*: $t = 1.62$, $p = 0.12$; *Females*: $t = 1.73$, $p = 0.089$). **E** As in (**A**) for the isolation-state preference (ISP) test (*Males*: $t = 2.73$ $p = 0.011$; *Females*: $t = 2.40$, $p = 0.021$). **F** As in (**A**) for the stress-state preference (SSP) test (*Males*: $t = 3.40$, $p = 0.0024$; *Females*: $t = 2.45$, $p = 0.0178$). ~ < 0.1, *$p < 0.05$, **$p < 0.01$, ***$p < 0.001$, ns – not significant; post hoc paired or unpaired t-test with FDR correction, following main effect in mixed-model ANOVA test

test stage, the mice (male and females pooled together) exhibited significantly higher investigation times compared to the pre-test stage (Additional file 1: Fig. S2A-D, SP: $F = 39.50$, $p < 0.001$; SxP: $F = 43.65$, $p < 0.001$; ISP: $F = 95.48$, $p < 0.001$; SSP: $F = 66.40$, $p < 0.001$; two-way repeated measures ANOVA), suggesting they had higher motivation to investigate stimulus-containing chambers compared to empty chambers. Additionally, the mice did not prefer any of the two empty chambers during the pre-test stage. However, during the test stage, we found a clear preference for one of the two stimuli: the social stimulus in the SP test, the opposite-sex stimulus in the SxP test, the isolated stimulus in the ISP test, and the stressed stimulus in the SSP test (Fig. 1C-F, *SP:* $F = 87.0$, $p < 0.001$; *SxP:* $F = 5.43$,

$p = 0.002$; *ISP:* $F = 11.51$, $p = 0.0011$; *SSP:* $F = 15.85$, $p < 0.001$; mixed-model ANOVA).

Further post hoc comparisons by sex revealed that both male and female subject mice displayed a clear preference in each test, except for the SxP test (Fig. 1C-F). Moreover, when considering the total time spent with each stimulus, males and females appeared to behave similarly across the different tests.

Analysing head acceleration data recorded during the behavioural tests

All recorded animals carried a wired head stage equipped with an accelerometer (Fig. 2A), which recorded raw 3D head acceleration data (Fig. 2B-D). Raw acceleration signals were processed using the pipeline described in Fig. 2E (see also Methods) to extract the overall dynamic (ODHA; Fig. 2F) and static (OSHA; Fig. 2G) head-acceleration components. Notably, while OSHA reflects the posture of the head, ODHA reflects its rapid movements. Raw signals derived from channels Y and Z were also processed, as described in Fig. 2H and G, to extract the head vertical Pitch and horizontal Roll, respectively (Fig. 2J-K).

To validate our analysis of the accelerometer recordings, we used the AI-based DeepLabCut (DLC) video analysis of pose estimation [39] to automatically extract the position of the two ears, the nose and the neck of the recorded mouse. We calculate the mean head speed from this dataset, which we defined as the average speed of these four head parts (Fig. 2L-M). As apparent in Fig. 2M, illustrating a representative 5-s segment of DLC speed traces, despite smoothing the data (see Methods), we encountered many instances of missing data (black arrows) due to low likelihood values (> 90%) (Additional File 1: Fig. S3A). These gaps sometimes affected individual head parts, while at other times, all tracked head parts were simultaneously lost (Fig. 2M, black arrows). Additionally, even with a likelihood threshold set at 90%, spurious peaks were observed (red arrow), likely due to inaccurate tracking of the head parts. These issues highlight the challenges in maintaining robust and reliable DLC tracking throughout the session.

Additionally, we used the distance between the nose and the neck to approximate the head Pitch (Fig. 2N-O) and the distance between the ears to approximate the head Roll (Fig. 2P-Q). Generally, these distances are inversely related to the Pitch and Roll (i.e., increased distance = decreased Pitch or Role), although this relationship may be affected by the viewing angle.

Typical movement of the head when approaching or leaving a stimulus

After establishing our analysis pipeline, we compared the head acceleration and DLC data by examining the animal's head kinematic variables at defined behavioural events along the test stage. For that, we analysed the data around the time points when the subject mouse started investigating a given stimulus or moved away from it (Fig. 3A), henceforth termed the start and end of the investigation bout, respectively. We analysed the data around these events by Z-scoring the signals across two seconds before and two seconds after each event (start or end of the investigation bout), using the first second of this time window as a baseline. To reduce noise and ensure that the mice were genuinely engaged in interaction, we analysed only investigation bouts lasting at least two seconds.

We revealed a significant difference in OSHA between the start and end of investigation bouts (Fig. 3B, OSHA: $F = 137.8$, $p < 0.001$, two-way mixed-model ANOVA). At the start of a bout, OSHA initially increased as the mouse approached the chamber and returned to baseline two seconds later, then decreased. In contrast, at the end of a bout, OSHA increased only after the subject detached from the chamber. Furthermore, the Roll and Pitch each displayed a unique pattern, which was inversely related to the distance between the nose and neck and the distance between the ears, respectively (Fig. 3C-F). Roll increased during the approach phase and decreased during the leaving phase (Fig. 3C, Roll: $F = 135.6$, $p < 0.001$; two-way mixed-model ANOVA), suggesting that subject mice turned their heads while approaching the stimuli and straightened their heads while leaving the chamber. Accordingly, the distance between the ears decreased during the start of investigation bouts, corresponding to a tilted head position along the Roll axis, while it was increased during leaving, as the head straightened (Fig. 3D, note the inverse Y-axis, Distance between ears: $F = 19.17$, $p < 0.001$; two-way mixed-model ANOVA).

As for the Pitch, we found a statistically significant interaction with time (Fig. 3E, Pitch: Event*Time, $F = 11,84$, $p < 0.001$; two-way mixed-model ANOVA). During the approach phase, there was an increase in the Pitch derived from the vertical Y-axis of the accelerometer. Thus, the mouse lowered or raised its head while approaching the stimulus and straightened it after about one second. This observation was not paralleled by the DLC analysis, where no significant change is observed between the approach phase compared to the leaving phase (Fig. 3F, note the inverse Y-axis, Distance nose to neck: Event*Time, $F = 2.87$, $p = 0.061$; two-way mixed-model ANOVA). Finally, the ODHA, capturing energy expenditure by rapid movements, was higher during the

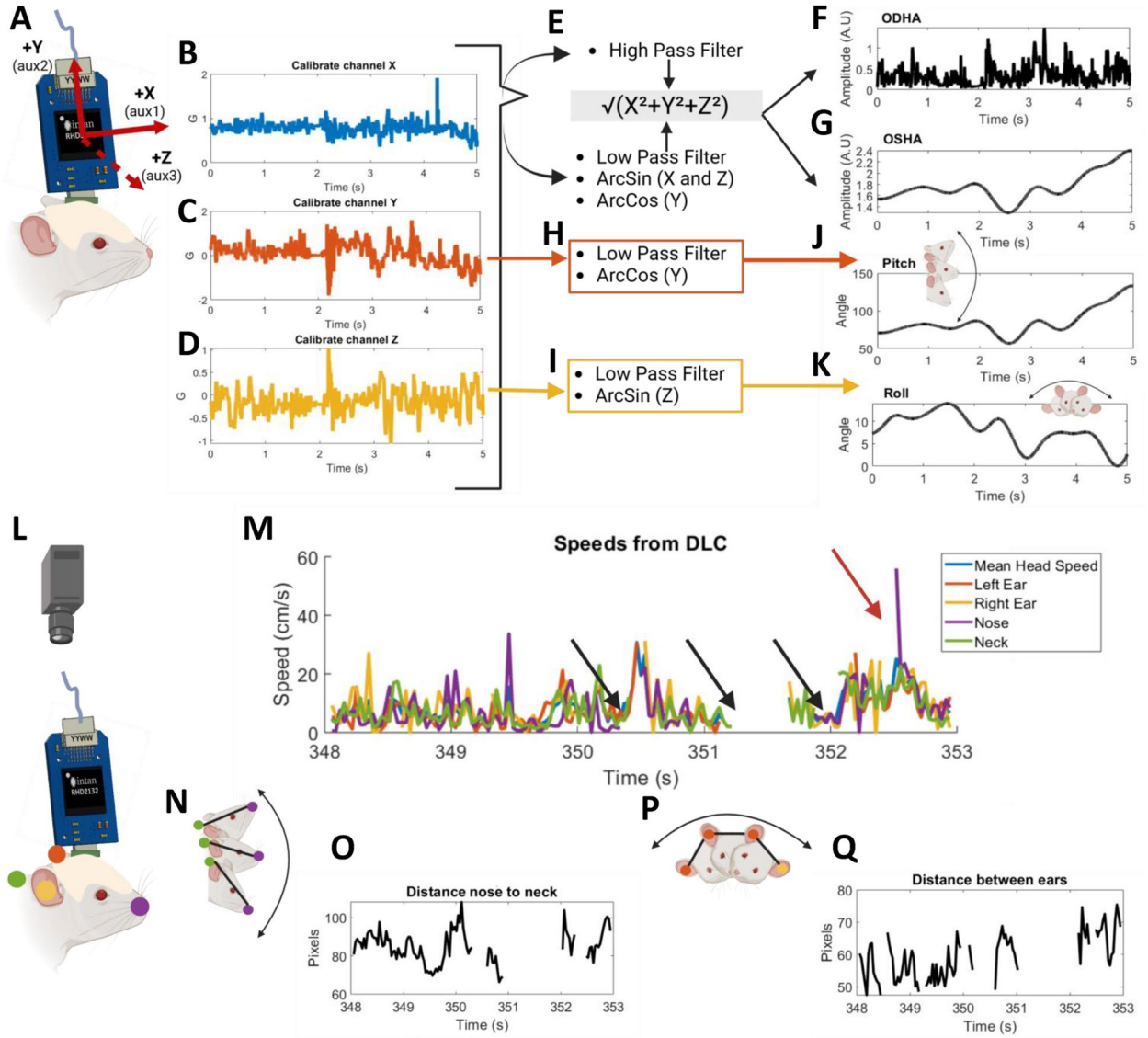

Fig. 2 Recording and calculating head kinematic variables using acceleration and video data. **A** Schematic representation of a mouse head with a head stage containing an accelerometer, illustrating the directions of the three axes (x, y, z). **B**-**D** Examples of 5-s long calibrated signals for the x-axis (**B**), y-axis (**C**), and z-axis (**D**). **E** Signal processing pipeline for the ODHA and OSHA: the square root of the squared sum applied to the low-pass filtered signals, followed by an ArcSin transformation (for the X and Z axes) or an ArcCos transformation (for the Y axis), yields the static component (OSHA). Applying the same operation to the high-pass filtered signals yields the dynamic component (ODHA). **F-G** Examples of 5-s traces for ODHA (**F**) and OSHA (**G**), representing the 3D dynamic and static components, respectively. **H-I** Signal processing pipeline for extracting Pitch and Roll angles from the raw y-axis and z-axis signals, respectively: a low-pass filter is applied, followed by an ArcCos transformation for the Y-axis (**H**) and an ArcSin transformation for the Z-axis (**I**). **J-K** Examples of 5-s traces showing pitch (**J**) and roll (**K**) angles, with accompanying schematics illustrating the corresponding head movements. **L** Schematic representation of a mouse head with DLC-labeled key points: left ear (orange), right ear (yellow), nose (purple), and neck (green). **M** Example of 5-s long speed traces for the four labelled head points, along with the mean head speed. The black arrows indicate missing data, and the red arrow indicates an anomalous peak caused by wrong nose tracking. **N-P** Schematic representation of the distance between nose and neck **(N)** and between the ears (**P**). **O-Q** Example of 5-s long traces of the distance between nose to neck (**O**) and ear-to-ear (**Q**)

end of bouts than at its start (Fig. 3G, ODHA: $F = 5.25$, $p = 0.026$). A similar pattern was observed in DLC-derived head speed data (Fig. 3H, Head speed: $F = 487.12$, $p < 0.001$; two-way mixed-model ANOVA, see Additional file 1: Fig. S3B-E for each head part). Thus, both accelerometer and DLC data yielded comparable results when analysing the head kinematic variables during the start and end of investigation bouts across all sessions.

To further validate our accelerometer data analysis, we trained a Random-forest model to classify the behaviour of the animal as either "approaching" or "leaving" according to the head kinematic variables measured during the second before the animal touched the stimulus chamber at the start of the investigation bouts or detached from it at the end of the bouts. The accelerometer data-based model correctly classified 60% of the approaching data and 57% of the leaving data, with results significantly higher than random distribution (Fig. I, Approaching: $\chi^2 = 66.76$, $p < 0.001$; Leaving: $\chi^2 = 70.78$, $p < 0.001$, Chi-square test). In contrast, the DLC-based model correctly recognised 80.86% of leaving events but only 34.10% of approaching events, which was worse than random. This result, which was significantly different from the random distribution (Fig. 3J, Approaching: $\chi^2 = 54.48$, $p < 0.001$; Leaving: $\chi^2 = 71.71$, $p < 0.001$, Chi-square test), indicates that the DLC-based model overfits the "Leaving" label. Thus, the model trained on the accelerometer data outperformed the DLC-based model.

Overall, these results validate the efficiency of our accelerometer data analysis pipeline as a tool for analysing head kinematics during social interactions without the data loss characterising DLC analysis.

Both dynamic and static head acceleration variables change profiles during social interaction

We then analysed the changes in the various head kinematic variables along the multiple stages of each 15-min session (pre-test, test and post-test; see Fig. 1A) separately for male and female mice. We found that the head-acceleration-based variables (Fig. 4A-H) and the DLC-based variables (Additional file 1: Fig. S4A-F) all exhibited significant changes between the various stages of the session, as detailed below.

ODHA and head speed were both higher during the test, as compared to pre- and post-test (Fig. 4A-B and Additional file 1: Fig. S4A-B; ODHA: $F = 103$, $p < 0.001$; Head speed: $F = 44.27$, $p < 0.001$), indicating that the mice exhibited faster head movements during the test. Interestingly, ODHA and head speed peaked around the introduction or removal of stimuli, suggesting a dependence of the head movement on the subject's arousal/alertness level (Fig. 4A, Additional file 1: Fig S4A).

A mean increase in the OSHA signal was observed during the test, as compared to the pre-and post-test stages (Fig. 4C-D; OSHA: $F = 13.19$, $p < 0.001$, two-way mixed-model ANOVA). This suggests that mice adopted head tilts with greater amplitude during the test, as supported by the results for Roll and Pitch. Specifically, Roll increased during the test (Fig. 4E-F; $F = 91.8$, $p < 0.001$), indicating that mice rolled their heads in a more robust manner during that period. A similar change was observed for Pitch (Fig. 4G-H; $F = 22.14$, $p < 0.001$, two-way mixed-model ANOVA), indicating greater vertical head tilts during the test stage. The Roll change was paralleled by an inverse change in the distance between ears, while the Pitch change was paralleled by the distance between the neck and nose (Additional file 1: Fig. S4C-F; Distance between ears: $F = 6.22$, $p = 0.002$; Distance nose to neck: $F = 46.22$, $p < 0.001$ two-way mixed-model ANOVA).

Besides changes between the various stages, some of the head kinematic variables also varied between the sexes in a statistically significant manner. While OSHA, Roll and Pitch did not vary between males and females (Fig. 4C-H), ODHA exhibited significant sex-dependent differences (Fig. 4AB; ODHA: $F = 6.49$, $p = 0.011$, two-way mixed-model ANOVA). Notably, males exhibited a higher ODHA signal than females, specifically during

(See figure on next page.)

Fig. 3 omparison of head kinematics at the start and end of investigation bouts between accelerometer and DLC data. **A** Schematic representation of the mouse starting and ending an interaction. **B** Mean Z-score of OSHA two seconds before and two seconds after the start (red) and end (green) of investigation bouts across all sessions. Time 0 represents the start of the bout; the baseline was defined as the interval from −2 to −1 s. Post hoc Wilcoxon tests with FDR correction were performed following a main effect in two-way mixed-model ANOVA (from −1 to 0 s: $W = 14{,}380$, $p < 0.001$; from 0 to 1 s: $W = 18{,}240$, $p < 0.001$; from 1 to 2 s: $W = 14{,}310$, $p < 0.001$). **C** Mean Z-score of the Roll signal, as in (**A**). Post hoc Wilcoxon tests with FDR correction were performed following a main effect in two-way mixed-model ANOVA (from −1 to 0 s: $W = 7210$, $p < 0.001$; from 0 to 1 s: $W = 614$, $p < 0.001$; from 1 to 2 s: $W = 734$, $p < 0.001$). **D** Mean Z-score of the Distance between ears, as in **(A).** Post hoc Wilcoxon tests with FDR correction were performed following a main effect in two-way mixed-model ANOVA (from −1 to 0 s: $W = 10{,}090$, $p < 0.001$; from 0 to 1 s: $W = 11{,}400$, $p < 0.001$; from 1 to 2 s: $W = 11{,}020$, $p < 0.001$). **E** Mean Z-score of the Pitch signal, as in (**A**). Post hoc Wilcoxon tests with FDR correction were performed following a main effect in two-way mixed-model ANOVA (from −1 to 0 s: $W = 13{,}660$, $p < 0.001$; from 0 to 1 s: $W = 15{,}670$, $p = 0.0013$; from 1 to 2 s: $W = 15{,}860$, $p = 0.0021$). **F** Mean Z-score of the Distance from nose to neck, as in (**A**). **G** Mean Z-score of the ODHA signal is as in (**A**). Post hoc Wilcoxon tests with FDR correction were performed following a main effect in two-way mixed-model ANOVA (from 0 to 1 s: $W = 8468$, $p < 0.001$; from 1 to 2 s: $W = 12{,}300$, $p < 0.001$). **H** Mean Z-score of Head Speed is as in (**A**). Post hoc Wilcoxon tests with FDR correction were performed following a main effect in two-way mixed-model ANOVA (from 0 to 1 s: $W = 2$, $p < 0.001$; from 1 to 2 s: $W = 1$, $p < 0.001$). **I-J** Confusion matrices for a binary Random Forest classifier predicting the type of event from the accelerometer (**I**) or DLC data (**J**) during the test. The accuracy scale is shown on the right. Percentages from each ground truth label are displayed at the center of each cell. Chi-square test ~ $p < 0.1$, *$p < 0.05$, **$p < 0.01$, ***$p < 0.001$, ns – not significant

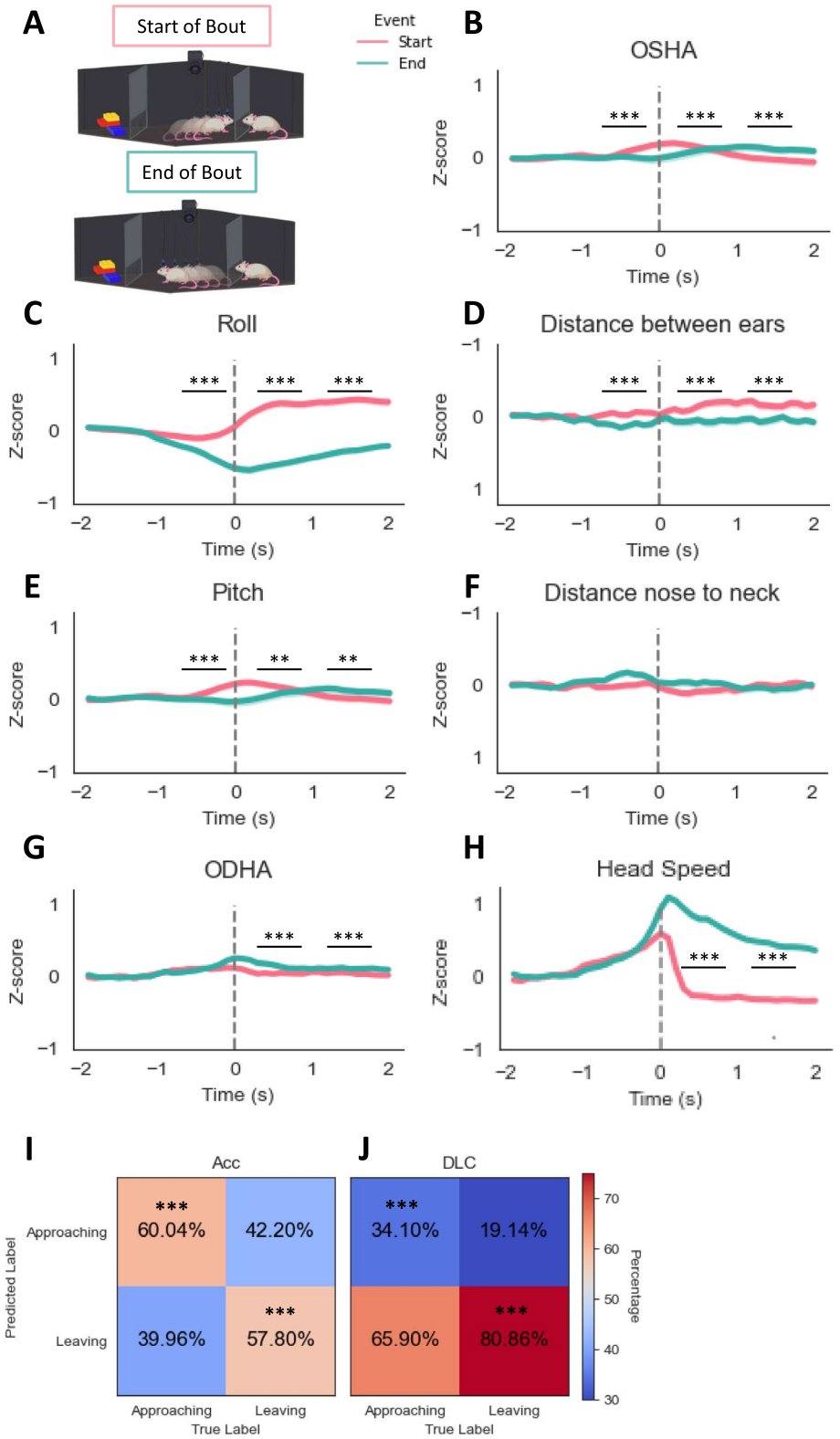

Fig. 3 (See legend on previous page.)

the test (Fig. 4A-B), suggesting that the dynamic component of head acceleration is sex-specific and dependent on the social context.

In contrast to the head acceleration-based results, the only sex-dependent difference observed in the DLC-based variables was in the distance between ears (Additional file 1: Fig. S4C-D; $F = 13.04$, $p < 0.001$; two-way mixed-model ANOVA). As this difference was slight and consistent across all the session stages, it most likely reflects the larger size of males compared to females. This highlights a limitation of using DLC with a single camera for monitoring head kinematics across various sexes and strains.

To investigate this issue further, we trained two separate random forest models to classify the subject's sex using the accelerometer or DLC data recorded during the test stage. The accelerometer-based model achieved an overall accuracy of 0.80, demonstrating strong performance in classifying both male and female subjects (Fig. 4I). Statistical analysis showed significant predictions for both females ($\chi^2 = 4.12$, $p = 0.042$, Chi-square test) and males ($\chi^2 = 4.95$, $p = 0.026$). In contrast, the DLC-based model showed a lower general accuracy of 0.75 (Fig. 4J), which most probably relied on the size differences between the sexes rather than on differences in head kinematics. Although these results approached statistical significance, the observed distributions did not differ significantly from the expected for both females ($\chi^2 = 2.7$, $p = 0.1$) and males ($\chi^2 = 2.68$, $p = 0.1$).

Overall, these results underscore the influence of sex and social context on the different components of head acceleration during social interactions. They also indicate that while accelerometer data provide a robust sex classification, DLC data did not achieve statistical significance. Therefore, our further analyses focused only on the accelerometer data.

Head acceleration dynamics during the social investigation are affected by the social context, stimulus attractiveness and the subject's sex

Next, we analysed head acceleration while subject mice investigated each of the two chambers containing the stimuli. To that end, we extracted the four head kinematic variables—ODHA, OSHA, Roll, and Pitch—specifically during the investigation bouts toward a given stimulus, normalised to bout duration. To filter out noise and ensure genuine engagement, only investigation bouts lasting longer than two seconds were included. Notably, we conducted the same analysis during the pre-test stage, when the subjects investigated empty chambers, and compared the results between the two stages (pre-test and test) separately for each behavioural test.

We observed a main effect of the stage for all four variables (Additional file 1: Fig. S5A-D; ODHA: $F = 144.93$, $p < 0.001$; OSHA: $F = 21.44$, $p < 0.001$; Roll: $F = 102.6$, $p < 0.001$; Pitch: $F = 29.61$, $p < 0.001$; two-way mixed-model ANOVA). Post hoc analysis revealed higher values of ODHA, Roll, and Pitch signals during stimulus investigation (test stage), as compared to empty chamber investigation (pre-test stage), across all behavioural tests (Additional file 1: Fig. S5ACD). For the OSHA signal, the difference was significant in all tests besides the SP test (Additional file 1: Fig. S5B). Overall, we observed more dynamic head movement and stronger head tilt during the investigation of stimulus-containing chambers than empty chambers. Given the higher investigation time observed during the test stage, compared to the pre-test stage, these results suggest that the four head kinematic variables are positively influenced by the motivation of the subject to investigate the chamber.

When comparing the signals recorded during stimulus investigation across different tests, a main effect of test type was observed specifically for the Roll signals (Fig. 5A; Roll: $F = 4.07$, $p = 0.007$; two-way mixed-model

(See figure on next page.)

Fig. 4 Sex-dependent changes in head kinematics along the session. **A** Change in the ODHA signal during the full 15 min for males (purple) and females (green), combining data from all tests. **B** Quantification of the ODHA signal changes, comparing sex and stages (pre-test, test, and post-test). Post hoc analysis following a main effect in two-way mixed-model ANOVA for Stage: Pre-test vs test ($W = 3842$, $p < 0.001$), test vs. post-test ($W = 7482$, $p < 0.001$), and pre-test vs. post-test ($W = 1276$, $p < 0.001$) (Wilcoxon test with FDR correction); and for Sex: test ($W = 7482$, $p = 0.007$) (Mann–Whitney-Wilcoxon test with FDR correction). **C** Same as (**A**) for the OSHA signal. **D** Same as (**B**) for the OSHA signal. Post hoc analysis following a main effect in two-way mixed-model ANOVA for Stage: pre-test vs. test ($W = 12{,}580$, $p < 0.001$), test vs. post-test ($W = 13{,}120$, $p < 0.001$) (Wilcoxon test with FDR correction). **E** Same as (**A**) for the Roll signal. **F** Same as (**B**) for the Roll signal. Post hoc analysis following a main effect in two-way mixed-model ANOVA for Stage: pre-test vs. test ($W = 5384$, $p < 0.001$) and test vs. post-test ($W = 5399$, $p < 0.001$) (Wilcoxon test with FDR correction). **G** Same as (**A**) for the Pitch signal. **H** Same as (**B**) for the Pitch signal. Post hoc analysis following a main effect in two-way mixed-model ANOVA for Stage: pre-test vs. test ($W = 10{,}820$, $p < 0.001$) and test vs. post-test ($W = 10{,}780$, $p < 0.001$) (Wilcoxon test with FDR correction). **I** Confusion matrices for a binary Random Forest classifier predicting sex from accelerometer-derived data across all tests during the 5 min of the test stage. Percentages for each category are displayed at the center of each cell (Chi-square test). The accuracy scale is shown on the right. **J** Confusion matrices for a binary Random Forest classifier predicting sex from DLC-derived data across all tests during the 5 min of the test stage. Percentages for each category are displayed at the center of each cell (Chi-square test). The accuracy scale is shown on the left. ~ $p < 0.1$, * $p < 0.05$, ** $p < 0.01$, *** $p < 0.001$, ns – not significant

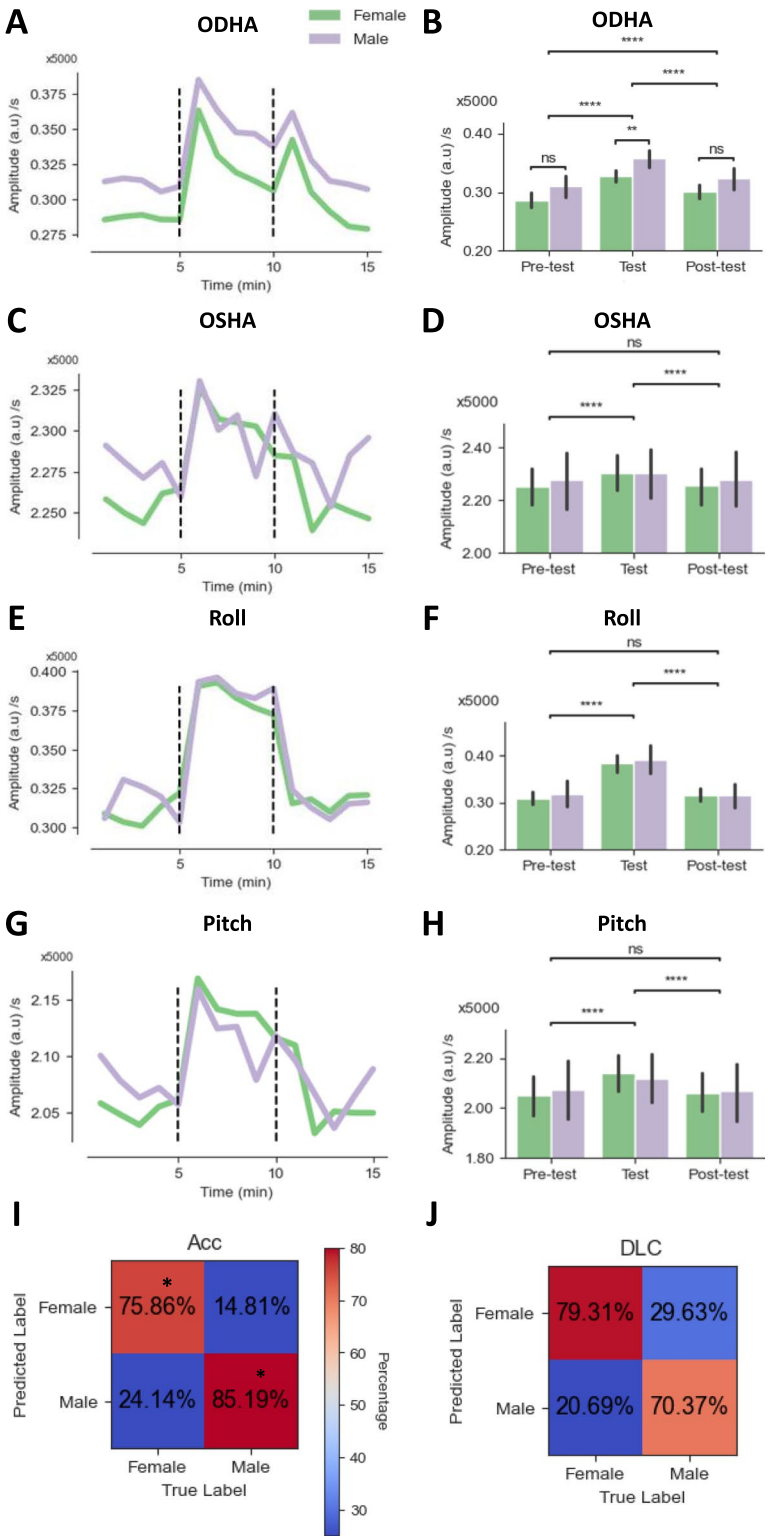

Fig. 4 (See legend on previous page.)

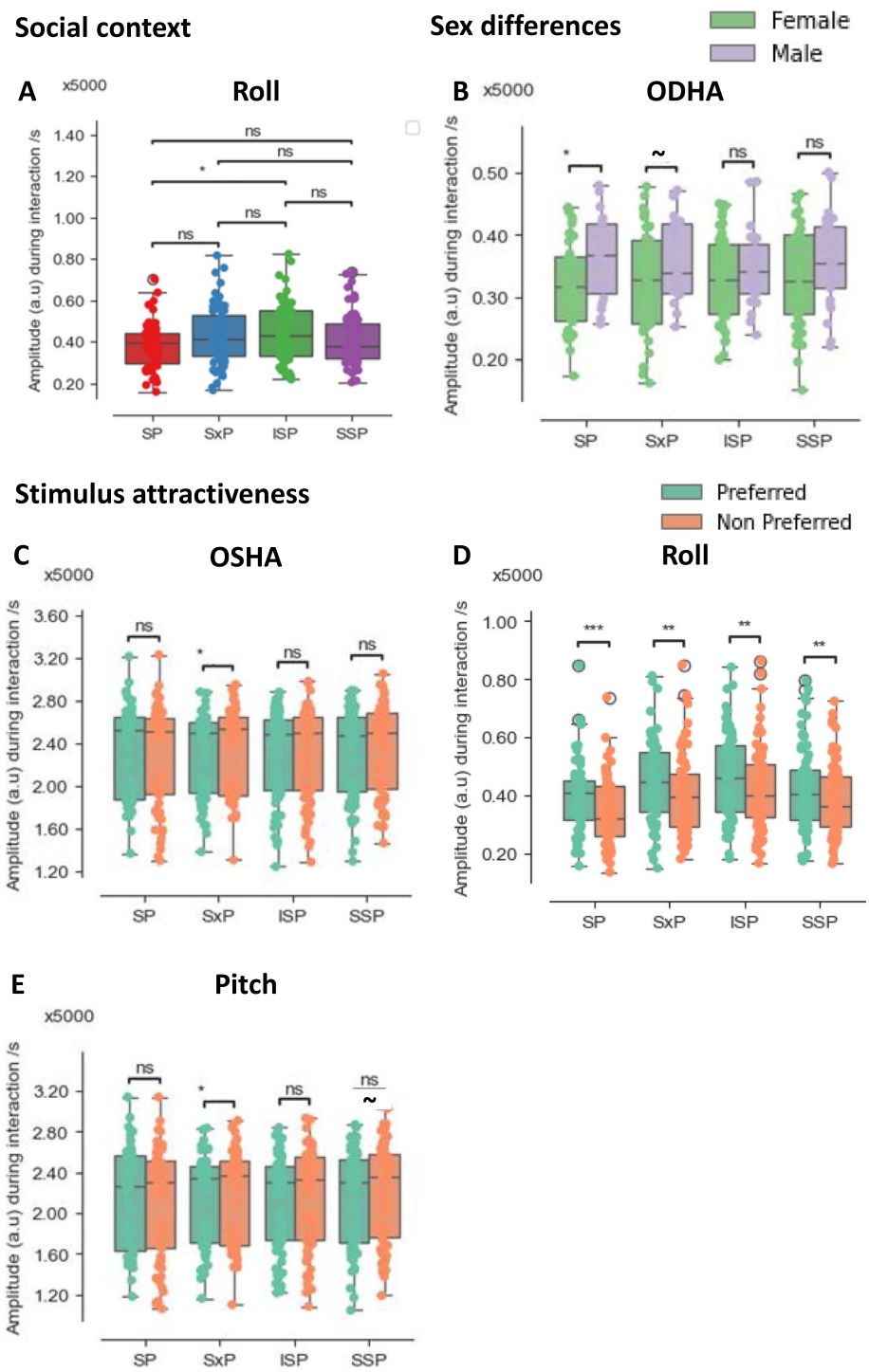

Fig. 5 Head kinematics during social investigations are affected by the social context, subject's sex and stimulus attractiveness. **A** Comparison between tests of the mean Roll signal amplitude during stimulus investigation. Post hoc paired Mann–Whitney-Wilcoxon test with FDR correction, following a main effect in the Kruskal–Wallis test (*SP-ISP*: $U = 1722$, $p = 0.024$). **B** Comparison between tests of the mean ODHA signal amplitude during stimulus investigation. Post hoc independent *t*-test with FDR correction, following a main effect in the mixed-model ANOVA (*SP*: $t = 2.188$, $p = 0.032$; *ISP*: $t = 3.645$, $p < 0.001$). **C** Comparison of the mean amplitude of the OSHA signal measured during stimulus investigation between preferred and non-preferred stimuli across all tests. Post hoc paired *t*-test with FDR correction, following a main effect in the mixed-model ANOVA (*SxP*: $t = -2.48$, $p = 0.015$). **D** As in (**C**), for the roll signal. Post hoc paired *t*-test with FDR correction, following a main effect in the mixed-model ANOVA (*SP*: $t = 3.56$, $p < 0.001$; *SxP*: $t = 2.91$, $p < 0.001$; *ISP*: $t = 3.02$, $p = 0.003$. *SSP*: $t = 2.82$, $p = 0.006$). **E** As in (**C**), for the pitch signal. Post hoc paired *t*-test with FDR correction, following a main effect in the mixed-model ANOVA (*SxP*: $t = -2.42$, $p = 0.017$). ~ $p < 0.1$, $p < 0.05$, * $p < 0.01$, ** $p < 0.001$, ns – not significant

ANOVA), with lower Roll values during the SP test compared to the ISP test. Notably, the SP test features the most diverse stimuli (a stimulus animal vs. a Lego toy) of all tests. Thus, the social context (test type) influenced the amplitude of head tilt in mice.

We then examined if head acceleration during stimulus investigation was sex-specific or sensitive to the attractiveness of the stimulus (preferred vs. non-preferred). When a two-way ANOVA was applied to compare the sexes across all four tests, separately for each variable, only the dynamic component (ODHA) was found significant (Fig. 5B, $F=9.12$, $p=0.002$; two-way ANOVA). A post hoc analysis revealed that females exhibited lower ODHA values during stimulus investigation than males, with significant differences in the SP test and a trend in the SxP test (Fig. 5B).

In contrast, stimulus preference influenced the OSHA (Fig. 5C), Roll (Fig. 5D), and Pitch (Fig. 5E) signals. We found a main effect of the stimulus on the Roll signal (Roll: $F=37.85$, $p<0.001$; two-way mixed-model ANOVA). There was also a significant interaction between stimulus and test type for the OSHA and Pitch signals (OSHA: Stimulus**Test*, $F=3.36$, $p=0.019$; Pitch: *Stimulus*Test*, $F=3.15$, $p=0.025$; two-way mixed-model ANOVA). Post hoc analyses revealed that mice exhibited higher Roll values while investigating the preferred stimulus compared to the non-preferred one in all tests. However, OSHA and Pitch values were higher when investigating the non-preferred stimulus during the SxP test.

Overall, the static, dynamic, and Roll components of head acceleration during stimulus investigation were influenced by distinct factors. OSHA, Roll and Pitch were affected by the level of stimulus attractiveness, and Roll was also influenced by the test type, whereas ODHA was influenced by the subject's sex. Specifically, males demonstrated more energetic movements (ODHA) during stimulus investigation than females. These findings suggest that mouse head movement patterns during stimulus investigation are shaped by both the sex of the subject and the attractiveness of the stimulus.

Social context-dependent head acceleration during the start and end of social investigation bouts

Since the subject mice conducted investigation bouts both before the test toward empty chambers and during the test toward stimulus-containing chambers, we examined if the presence of a stimulus in the chamber elicited a change in the way by which the subject started or ended investigating the chamber (pulling males and females together). Using Z-score analysis as described above, we found that out of the four kinematic variables, only ODHA and Roll showed such changes (Fig. 6). The ODHA exhibited significant differences between the stages only at the start of investigation bouts (Fig. 6A-B; *Stages*Time*, $F=4.37$, $p=0.015$), Unexpectedly, the ODHA level at the start of bouts was lower during the test than during the pre-test stage, suggesting less energetic movements while approaching stimulus-containing chambers, compared to empty chambers. This may reflect a certain level of caution exhibited when the subject approaches a novel stimulus in a chamber.

In contrast to ODHA, Roll exhibited pronounced differences between stages at both the start and end of bouts, with a significant interaction between stage and time at the beginning of the bout and a main effect of stage at the end of the bout (Fig. 6E, F; Start: *Time*Stage: $F=19.39$, $p<0.001$;* End: $F=2103$, $p<0.001$; two-way repeated measures ANOVA). In both the start and end of the bout, the Roll signal exhibited stronger changes during the test stage than during the pre-test stage. This suggests that subjects exhibited stronger head rolling while approaching and leaving stimulus-containing chambers, as compared to empty chambers.

Overall, these results suggest that the general social context, i.e., the presence of stimuli in the chambers during the test stage, significantly affects the head kinematics at the beginning and end of investigation bouts.

Sex-dependent head acceleration during the start and end of social investigation bouts

As discussed earlier, males exhibited a higher mean ODHA signal, as compared to females, throughout the entire session (Fig. 4A-B), as well as during stimulus investigation (Fig. 5B). We, therefore, analysed the head kinematic variables, specifically at the start and end of stimulus investigation bouts.

Interestingly, we found a significant sex-dependent difference in ODHA at the start of the investigation of the empty chambers during the pre-test stage, with males showing a greater increase in acceleration than females (Fig. 7A; $F=5.03$, $p=0.033$; two-way mixed-model ANOVA). This difference emerged one second before the start of the bout and persisted for at least two seconds. However, during the test stage, this pattern disappeared (Fig. 7B). At the end of the bout, the opposite was observed: there was no difference between males and females when leaving an empty chamber (Fig. 7C). However, a difference emerged when leaving the chamber during the test, with a significant interaction between time and sex (Fig. 7D; Sex*Time: $F=3.62$, $p=0.033$; two-way mixed-model ANOVA). Specifically, one second before detaching from the chamber, males exhibited greater movement compared to females, and this difference persisted until one second after leaving the chamber.

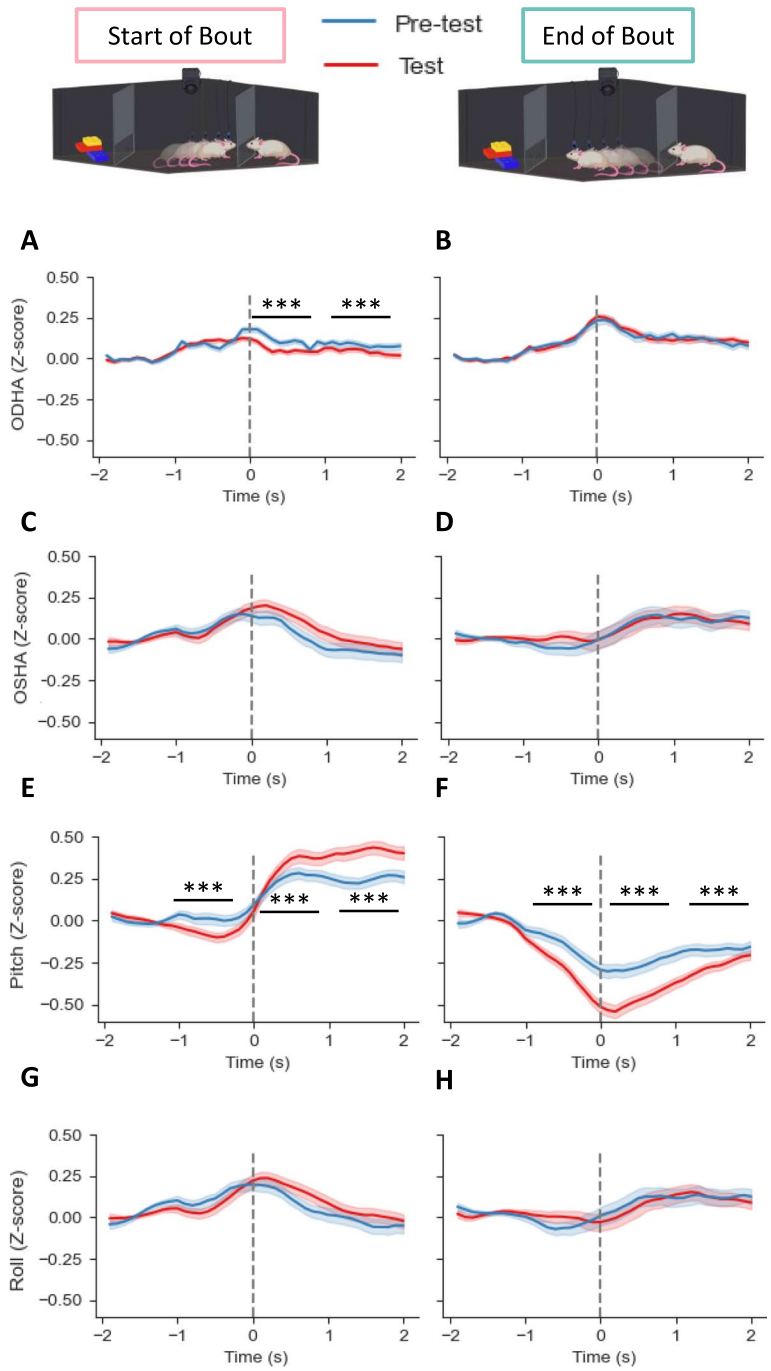

Fig. 6 Stage-dependent differences in mice head acceleration during the start and end of investigation bouts. **A** Mean traces (± SEM) of the Z-score during all tests and for both sexes are shown for the pre-test (blue) and test (red) stages for the ODHA signal at the start of investigation bouts. Time 0 represents the start of the bout; the baseline was defined as the interval from −2 to −1 s. Post hoc paired-t-test test with FDR correction, following main effect in two-way repeated measures ANOVA (*from 0 to 1 s:* t = 6.04, $p < 0.001$.; *From 1 to 2 secs:* t = 3.91, $p < 0.001$). **B** As in (**A**), for the end of all investigation bouts. **C** As in (**A**), for the OSHA signal. **D** As in (**B**), for the OSHA signal. **E** As in (**A**), for the Roll signal (*from −1 to 0 s:* t = 4.3, $p < 0.001$; f*rom 0 to 1 s:* t = —3.61, $p < 0.001$; *From 1 to 2 secs:* t = —7.787, $p < 0.0.01$). **F** As in (**B**), for the Roll signal (*from −1 to 0 s:* t = 8.3, $p < 0.001$; *from 0 to 1 s:* t = 9.88, $p < 0.001$; *From 1 to 2 secs:* t = 5.24, $p < 0.0.01$). **G** As in (**A**), for the Pitch signal. **H** As in (**B**), for the Pitch signal

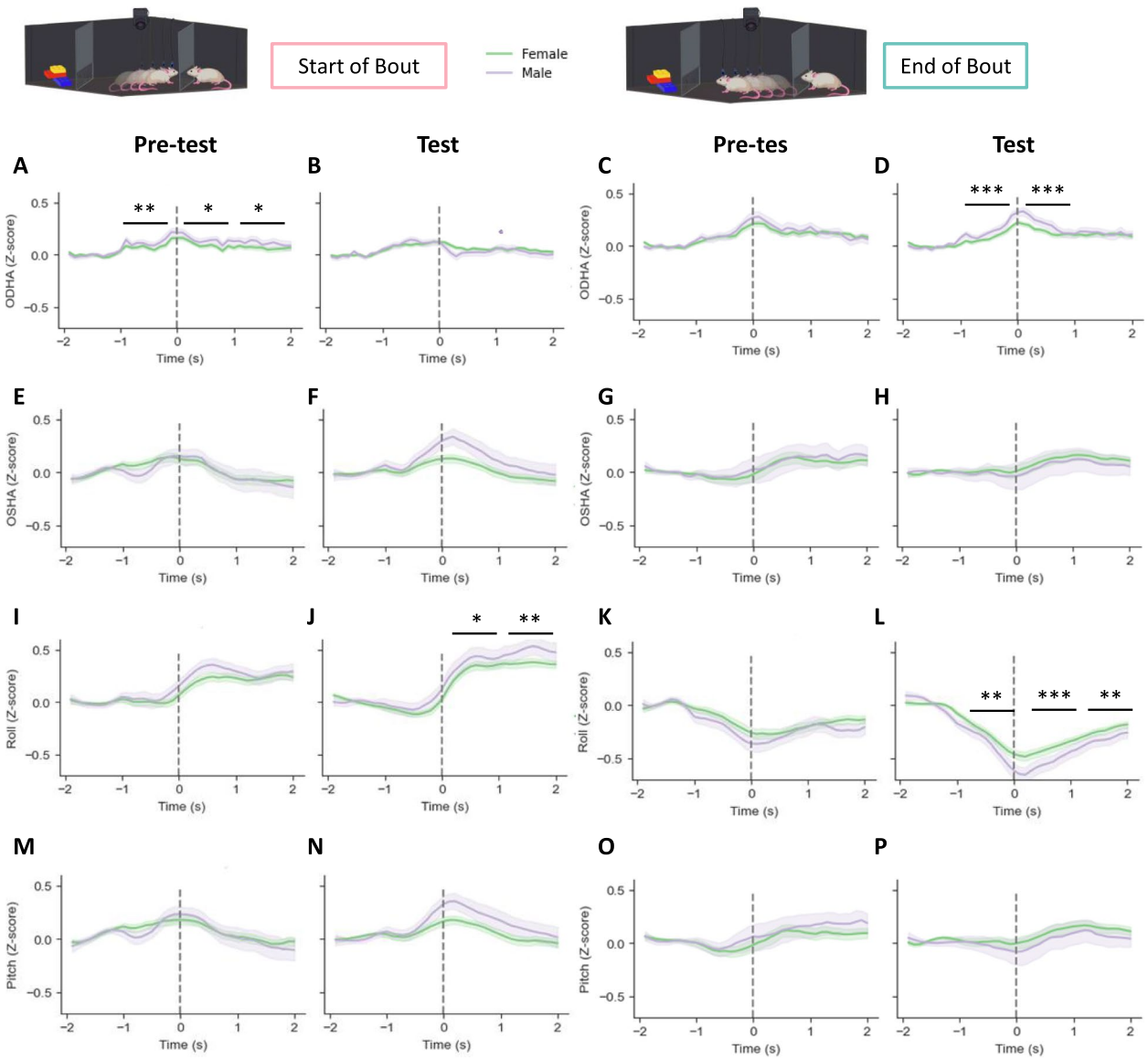

Fig. 7 Sex differences in head acceleration during the start and end of investigation bouts. **A** Mean traces (± SEM) of the Z-score of ODHA at the start of bouts during the pre-test stage, shown for male (purple) and female (green) mice across all tests. Time 0 represents the start of the bout, while the time from −2 to −1 s was considered as the baseline. Post hoc independent t-test independent with FDR correction, following main effect in two-way mixed-model ANOVA (*from −1 to 0 s*: t = —3, $p = 0.0029$; *from 0 to 1 s*: t = —3.24, $p = 0.0013$; *from 1 to 2 s*: t = —2.585, $p = 0.0102$). **B** As (**A**), for the ODHA signal at the beginning of bouts during the test stage. **C** As (**A**), for the ODHA signal at the end of bouts. **D** As (**B**), for the ODHA signal at the end of bouts (*from −1 to 0 s*: t = —4.68, $p < 0.001$; *from 0 to 1 s*: t = —3.66, $p < 0.001$). **E** As (**A**), for the OSHA signal. **F** As (**B**), for the OSHA signal. **G** As (**C**), for the OSHA signal. **H** As (**D**), for the OSHA signal. **I** As (**A**), for the Roll signal. **J** As (**B**), for the Roll signal (*from 0 to 1 s*: t = —2.07, $p = 0.039$; *from 1 to 2 s*: t = —3.03, $p = 0.0026$). **K** As (**C**), for the Roll signal. **L** As (**D**), for the Roll signal (*from −1 to 0 s*: t = 3.03, $p = 0.0026$; *from 0 to 1 s*: t = 3.92, $p < 0.001$; *from 1 to 2 s*: t = 3.018, $p = 0.0027$). **M** As (**A**), for the Pitch signal. **N** As (**B**), for the Pitch signal. **O** As (**C**), for the Pitch signal. **P** As (**D**), for the Pitch signal. ~ < 0.1, * $p < 0.05$, ** $p < 0.01$, *** $p < 0.001$, ns – not significant

While the Pitch signal showed no sex-dependent differences (Fig. 7M-P), a significant interaction between time and sex was observed for the Roll signal during the test stage at both the start and end of bouts (Fig. 7J and L; Start: F = 4.65, $p = 0.04$; End: F = 8.61, $p = 0.007$; two-way mixed-model ANOVA). Specifically, males exhibited a higher Roll signal during the first two seconds of interaction with the stimuli. At the end of the bout, males showed a greater decrease in Roll compared to females, starting one second before detaching from the stimulus-containing chamber and lasting until two seconds after. No difference was observed during the pre-test stage

(Fig. 7I and K), suggesting that these sex-dependent Roll signals depended on the presence of a stimulus in the chamber. For the OSHA signal, no significant sex-dependent differences were observed (Fig. 7E-H).

Mouse head movement at the beginning and end of investigation bouts varied according to stimulus attractiveness

Finally, we found that the mere presence of a stimulus in the chamber changed the head kinematics of the subject mice at the start and end of investigation bouts (Fig. 6). We next examined whether the mice adapted their head movements based on their preference for the investigated stimulus, pooling the results from all behavioural tests. Significant differences were observed between preferred and non-preferred stimuli across all kinematic variables derived from the accelerometer signals (Fig. 8). All head kinematics showed significant differences between the preferred and non-preferred subjects when starting or ending a bout (Fig. 8A-H), except for the Roll signal, where a strong tendency was found in ANOVA (Fig. 8F; ODHA: $F=3.68$, $p=0.055$; two-way repeated measures ANOVA).

The ODHA signal showed a significant interaction between Stimuli and Time at the start of bouts (Fig. 8A; ODHA: $F=6.18$, $p<0.001$; two-way repeated measures ANOVA). Specifically, the ODHA signal was higher when mice approached the non-preferred stimulus. However, from one to two seconds after reaching the stimulus, subjects exhibited stronger overall movement with the preferred stimulus compared to the non-preferred one, indicating a more energetic movement. Mice also displayed higher ODHA signals when leaving the non-preferred stimulus compared to the preferred one, from one second before detaching from the chamber to two seconds after (Fig. 8B; ODHA: $F=5.43$, $p=0.020$; two-way repeated measures ANOVA). The OSHA and Pitch signals followed a similar pattern. Both were significantly higher when mice approached the non-preferred stimulus compared to the preferred one (Fig. 8C, G; OSHA: $F=6.18$, $p=0.013$; Pitch: $F=9.6$, $p=0.002$; two-way repeated measures ANOVA). Conversely, when leaving the non-preferred stimulus, mice exhibited a lower amplitude for both OSHA and Pitch signals (Fig. 8D, H; OSHA: $F=6.32$, $p=0.012$; Pitch: $F=4.88$, $p=0.027$; two-way repeated measures ANOVA). As for the Roll signal, mice exhibited a significantly higher increase during the second seconds of interaction with the non-preferred stimulus (Fig. 8E; Roll: $F=4.61$, $p=0.03$; two-way repeated measures ANOVA).

Thus, a clear pattern emerged at the start of a bout: an increase in tilt and rolling negatively correlated with the mouse's interest in the stimulus. These patterns differed from those observed between stages (Fig. 6); the presence or absence of a stimulus affected movement differently than the preference between two stimuli. In contrast, both factors influenced the ODHA similarly. Overall, head acceleration at the start or end of an investigation bout appears to adjust to both the general social context and the attractiveness of the stimulus being investigated. These findings suggest that mice adapt their head posture and the energy expended in head movements based on both contextual conditions and the nature of the stimulus being evaluated.

Discussion

In this study, we utilised four variables derived from raw accelerometer data—ODHA, OSHA, Roll, and Pitch—to characterise and quantify head movements during murine social behaviour. ODHA approximates the energy expended on rapid head movements [17, 40, 41], while OSHA, defined here for the first time, provides information on the general amplitude of the head's movement across all three axes. Additionally, Roll and Pitch describe the amplitudes of horizontal roll and vertical pitch head movements, respectively. Since the yaw angle movements are unaffected by gravity, they cannot be extracted from the accelerometer data. Despite this limitation, these four measurements enabled us to provide a relatively precise description of head movements. They exhibited distinct and consistent patterns when examined at various time windows: across the entire session, during social investigations and at the start and end of investigation bouts. These patterns allowed us to successfully predict

(See figure on next page.)

Fig. 8 Context- and stimulus-specific adaptation of mouse head movements. **A** Mean traces (± SEM) of the Z-score during all tests and for both sexes are shown for preferred (red) and non-preferred (blue) stimuli for ODHA signal at the start of investigation bouts. Time 0 represents the start of the bout; the baseline was defined as the interval from −2 to −1 s. Post hoc paired-t-test test with FDR correction, following main effect in two-way repeated measures ANOVA (*from −1 to 0 s:* t = 2.42, $p=0.016$; *From 1 to 2 secs:* t = —2.18, $p=0.03$). **B** As in (**A**), for the end of all investigation bout (*from −1 to 0 s:* t = 3.83, *from 0 to 1 s:* t = 4.33, $p<0.001$; *from 1 to 2 secs:* t = 3.98, $p<0.001$). **C** As in (**A**), n for the OSHA signal (*from −1 to 0 s:* t = 3.13, $p=0.0018$; *from 0 to 1 s:* t = 2.14, $p=0.033$). **D** As in (**B**), for the OSHA signal. (*from −1 to 0 s:* t = −2.78, $p=0.0057$; *from 0 to 1 s:* W = 2.23, $p=0.03$; *From 1 to 2 secs:* W = 2.1, $p=0.036$). **E** As in (**A**), for the Roll signal (*From 1 to 2 secs:* W = 2.12, $p=0.034$). **F** As in (**B**), for the Roll signal (*From 0 to 1 secs:* W = 2, p = 0.046; *From 1 to 2 secs:* W = 2.1, $p=0.037$). **G** As in (**A**), for the Pitch signal (*from −1 to 0 s:* t = 3.62, $p<0.001$; *from 0 to 1 s:* t = 8.75, $p<0.001$). **H** As in (**B**), for the Pitch signal (*from 0 to 1 s:* t = —2.19, $p=0.0$é). ~ < 0.1, *$p<0.05$, **$p<0.01$, ***$p<0.001$, ns – not significant

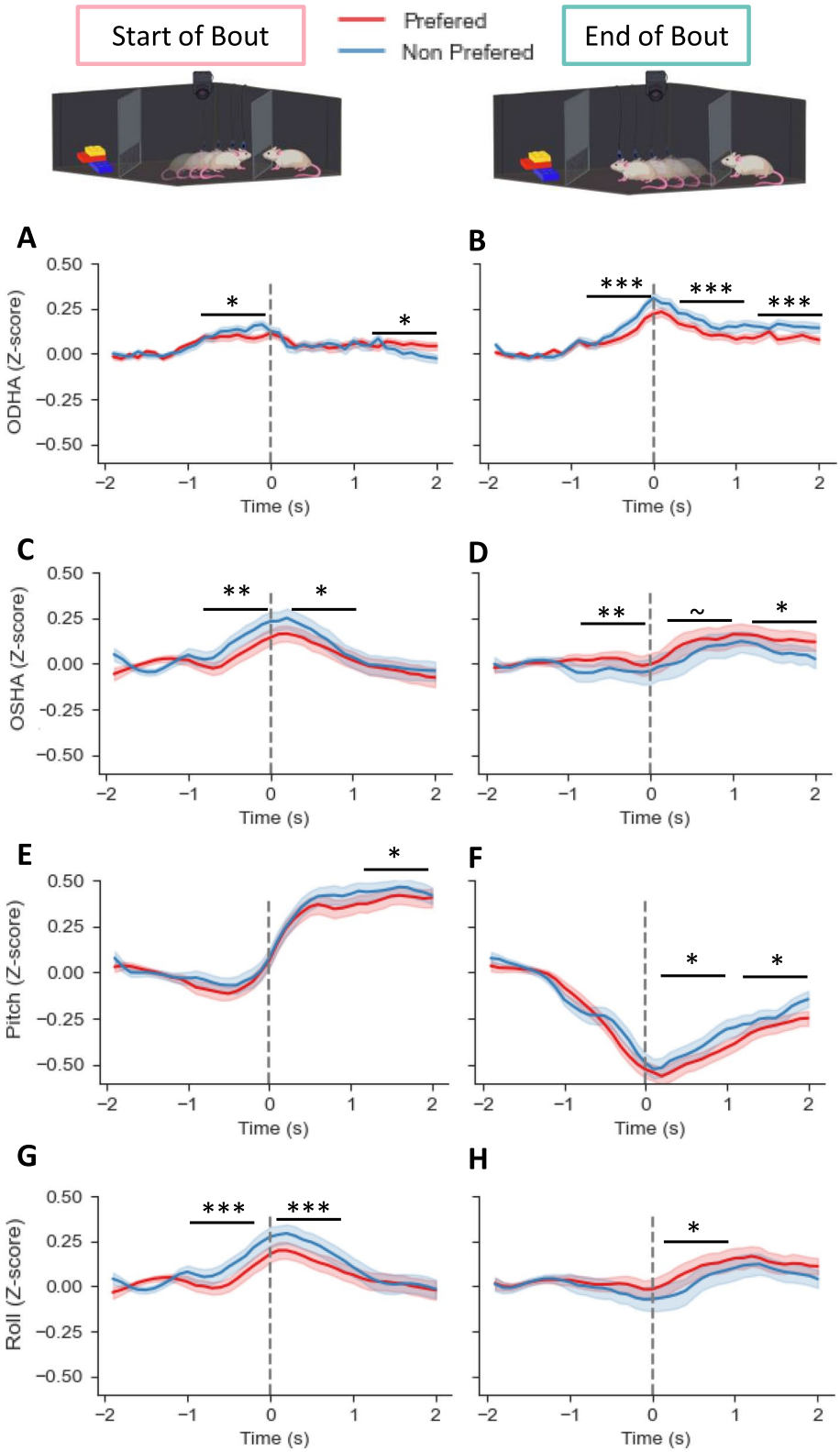

Fig. 8 (See legend on previous page.)

the sex of the subject, as well as whether the subject was approaching or leaving a stimulus.

The different variables complement each other, providing a comprehensive understanding of head movement. Such insight cannot be achieved by solely relying on body part velocities, as estimated from video analysis, even if a cutting-edge analysis such as DLC is used. Although we obtained consistent results using DLC, their predictive power was lower relative to the accelerometer data. This limitation may be due to occlusions, missing data, and sampling rate constraints. Thus, despite applying multiple levels of data filtering—including selecting frames with high likelihood scores and removing outliers, we only reached a partially coherent head-movement analysis using DLC. For example, the head speed extracted with DLC did not capture the differences between males and females observed in ODHA during the test stage. Moreover, while the distances between the ears or between the nose and neck can approximate Roll and Pitch, the relationship between these distances and their corresponding angles is inherently complex, especially when using a single fixed camera. Using two or three cameras could mitigate many of these issues, but this approach is both costlier and significantly more time-consuming to implement and analyse. Moreover, video-based analyses become increasingly challenging when tracking free interactions among multiple animals. In our experimental setup, additional constraints, such as the opaque arena, which precludes the addition of side cameras, and the head wiring that often obscures parts of the head, further complicate accurate DLC tracking. Additionally, the sampling rate of accelerometer data, which covers frequencies from 1 to 100 Hz, is much higher than the 30 frames per second typically captured by video cameras. This lower video frame rate limits the ability to capture high-frequency movements, thereby obscuring subtle behavioural nuances. Accelerometers provide a practical solution to these challenges, and they are often already integrated into headstages used for electrophysiology recordings and miniature microscopy systems like Inscopix.

When analysing the signals across the various session stages, we observed a significant and transient increase in the ODHA signal immediately after stimuli were either introduced or removed from the arena. This suggests that mice expend more energy on rapid movements of their heads during these periods when they are presumably alerted by the changes in their environment. Notably, a very similar pattern of transient increase around stimulus introduction and removal was reported for local field potential theta rhythmicity recorded from social behavior-associated brain regions of rats and mice [42, 43]. As theta rhythmicity in various brain areas is associated with arousal/alertness/attention states [44–50], as well as with active sensing [51], the ODHA may reflect rapid head movement during active sensing episodes elicited by alerting events, such as social stimuli introduction and removal.

Furthermore, while examining the ODHA over the entire session, we observed differences between males and females during the test but not during the pre- or post-test stages (Fig. 4). In the context of social interaction, males exhibited a greater increase in energy expenditure compared to females [52]. Accordingly, when analysing the mean ODHA per second during stimulus investigation, we found that males displayed a higher signal compared to females (Fig. 5). Although the investigation time for each stimulus did not differ between males and females, it appears that there are differences in how they interact with stimuli, specifically in terms of rapid head movements. We also observed differences between males and females during the test, at the start and at the end of the investigation bout for the Roll signal, as well as at the end of the bout for the ODHA signal. Although these differences were not large, they were consistent across different types of analyses. Thus, while measuring the time spent with each stimulus revealed no sex-dependent differences, the use of accelerometer data allowed us to detect more nuanced and subtle sex-dependent behavioural variations.

All four kinematic variables increased with the introduction of a general social context (Fig. 4, Additional file 1: Fig. S5). Roll varied throughout the investigation bout depending on the test type, suggesting that an animal's posture during stimulus interactions is influenced by the specific nature of the social context rather than merely by its presence. When analysing specific events, ODHA and Roll were the two most affected signals. Notably, Roll increased more when mice reached the stimulus-containing chamber during the test stage compared to the empty chamber during the pre-test stage, whereas ODHA showed the opposite pattern. Conversely, Roll exhibited a stronger decrease when mice left the chamber during the test compared to the pre-test stage (Fig. 6). Together, these findings, examined across different time scales, suggest that head movement reflects the subject's motivation to investigate the stimulus. Consistent with this interpretation, mice displayed greater movement amplitudes when interacting with the non-preferred stimulus compared to the preferred one across all four acceleration signals (Fig. 8), reflecting both static and dynamic components.

Overall, our results suggest that head acceleration provides valuable insights into the subject's affective and motivational states during social interactions. These findings are consistent with those reported in

human studies [53, 54]. Specifically, similar results have been observed in humans regarding the impact of motivation during interactions on the static component of accelerometer data. For example, by using a close measurement RMS of the angular displacement for pitch yaw, researchers found interpersonal coordination of head motion in distressed couples, which implies that humans change their angular displacement according to the emotion of the person with whom they interact [53]. Furthermore, regarding the link between arousal and accelerometer signals, similar findings have also been published in humans, where head movement can vary depending on the characteristics of the speaker or listener, such as their sex [55, 56]. Researchers also showed that it is possible to predict age from head movement patterns [57]. It would be interesting to explore additional intrinsic factors that influence these head movements in a social context, including age, as well as the mental and emotional conditions of the subject. Studies have shown motor deficiencies in several psychiatric disorders [58–60] linked to social deficits [61]. Researchers have been able to classify the severity of depression symptoms based on the velocity and acceleration of facial and head movements. Fournier et al. [62] showed that humans with ASD have altered motor control in posture, gait and praxis, producing decreased static and dynamic postural control during quiet stance. This movement impairment is also found in many rodent models of ASD. For example, VPA-treated rats (an ASD model) displayed greater movement acceleration, reduced distance between stops, and spent more time in the corner of the open-field arena [63]. Moreover, an article showed that by studying the proportion of time that the child approached or avoided the clinician and the direction that the child faced in relation to the clinician, they could explain 30% of the variance in ADOS (Autism Diagnostic Observation Schedule) score of ASD children [64]. It would be interesting to use an accelerometer in order to study these movement deficiencies in a social context. Investigating the relationship between impaired head movement and the integration of social cues in rodent models of psychiatric conditions could offer valuable insights into movement's role in pathological and physiological social decision-making processes.

Other applications of accelerometer data have already been started to be explored. For example, in a previous study, ODHA was used to extract reaction times in operant conditioning while conducting simultaneous multi-electrode recordings [65]. Future analyses could further enhance this approach. As our results show that accelerometer-based analyses effectively capture subtle differences in head movements, including preferences for specific stimuli, investigating correlations between these results and electrophysiological recordings would be a promising direction for future research.

Conclusion

Overall, head acceleration variables demonstrate clear responses to both the social context and the attractiveness of stimuli, highlighting their potential for assessing behavioural nuances during social interactions. Our findings suggest that these differences reflect varying levels of social motivation and/or alertness among mouse subjects in response to different social stimuli. Inertial measurements offer significant advantages over traditional observational methods, enabling more accurate detection of behavioural sequences and arousal states [22].

Our study provides a novel method and analysis pipeline for studying the social behaviour of small rodents in high-time resolution using a head-based accelerometer. We demonstrated the advantages of this method in standard video analysis and characterised how head kinematic variables change according to sex, social context, and motivation, suggesting that they may assist in monitoring the subject's affective state during social interactions.

Methods

Animals

The subjects for this study were adult male ($N=12$) and female ($N=22$) ICR (CD-1) mice, 2–3 months old, purchased from Envigo (Rehovot, Israel). Social stimuli were ICR juvenile mice (3–4 weeks old, used for the SP test only) or adult male and female mice similar to the subjects. All mice were kept within the SPF mouse facility of the University of Haifa at a temperature of 22 ± 2 °C in a reverse 12-h light–dark cycle (lights on at 7 am), with ad libitum access to a standard chow diet (Envigo) and water. Testing occurred during the dark phase under dim red-light conditions. The stimulus mice were group-housed, with 3–5 mice per cage. Post-surgery, subject mice were individually housed for about one week for recovery and were kept in individual housing until the end of the experiments in order to prevent damage to the implant. All experimental procedures were approved by the Institutional Animal Care and Use Committee of the University of Haifa (UoH-IL2203-139, 1077U).

Behavioural setups

The experimental setup was as previously described [66]. A black matte Plexiglas arena measuring $30 \times 22 \times 35$ cm housed two triangular structures (12 cm isosceles, 35 cm height). The bottoms of the triangular structures were covered with a metal mesh (18 cm × 6 cm; 1 cm × 1 cm holes). These triangular chambers were positioned in

two randomly selected opposite corners of the arena. The arena was placed in the center of an acoustic chamber, which was electrically shielded and grounded to the recording system via 2-mm aluminium plates. At the top of the chamber, a high-quality monochromatic camera (Flea3 USB3, FLIR – formerly Point Gray) was installed and connected to a computer. Video clips were recorded at 30 frames per second using FlyCapture2 software (FLIR).

Behavioural paradigm

All experiments took place during the dark phase of the light–dark cycle. Mouse subjects performed four different social discrimination tests: Social Preference (SP), Sex Preference (SxP), Isolation-State Preference (ISP), and Stressed-State Preference (SSP), as previously described [36, 37, 67]. The number of sessions and animals recorded and used for analyses for each test are indicated in Table 1 below.

During each test, we recorded the behaviour with a video camera and an accelerometer (see below). The stimulus animals were always novel to the subjects, with male stimuli presented to male subjects and female stimuli to female subjects, except for the SxP test. The stimuli used in the SP test included a novel group-housed juvenile mouse (social) and a Lego toy (object). In the SxP test, adult group-housed male and female mice served as stimuli. In the ISP test, adult isolated (for at least seven days) and group-housed mice were used as stimuli, while in the SSP test, stressed (placed in a perforated plastic 50-ml tube for 15 min before the test) and naive group-housed mice were used.

Before each test, subject mice were briefly exposed to isoflurane to prevent them from getting stressed while connecting the head stage to the implant. Habituation was performed for 10 min, allowing acclimation to the arena containing empty chambers before the recording started. The recording comprised three 5-min stages: a pre-test period with empty chambers at opposite corners of the arena, a test period with stimuli placed in the chambers, and a post-test stage with empty chambers.

Table 1 Number of mice and sessions per test

	Female		Male	
	Number of mice	Number of Sessions	Number of mice	Number of Sessions
SP	22	43	10	19
SxP	21	48	9	21
ISP	21	47	12	27
SSP	20	50	10	25

Each subject animal underwent testing twice a day for three consecutive days, with two sessions conducted in the morning and two in the afternoon. Each subject animal conducted each test three times (sessions) in a pseudo-randomized order (Fig. 1A). Sessions were excluded under specific conditions: 1) when the head stage or connector was detached from the subject's head; 2) in instances of a recording failure; 3) when the subject mouse engaged in less than two bouts of stimulus investigation (see Additional file 2: Table 1). An investigation bout is defined as the event starting with a touch between the subject and the stimulus chamber and ending after the subject detached from the chamber for > 2 s. These exclusions contributed to the observed variation in the number of sessions and subjects across different tests (see Table 1 below).

Surgery

Subject mice were anaesthetised via intraperitoneal injection of ketamine and Domitor mixture (at 0.13 mg/g and 0.01 mg/g, respectively). The depth of anaesthesia was regularly assessed by testing toe pinch reflexes and sustained using isoflurane administered through a low-flow anaesthesia system (0.5–1%, ~200 mL/min; SomnoFlo, Kent Scientific). A closed-loop custom-made temperature controller system was employed to maintain a constant body temperature of approximately 37 °C. During the procedure, the anaesthetised animals were securely positioned in a stereotaxic apparatus (Kopf Instruments, Tujunga, CA) with the head in a flat position. Following the removal of shaved skin, slow drilling into the skull was performed to implant two screws. A female Mill-Max connector (#853–43–100–10–001000), along with the screws, was fixed to the skull using dental cement in the alignment of the bregma and lambda. This female connector was then permanently connected to an adaptor (male Mill-Max connector, #852–10-004–10–001000, soldered to an 18-pin female Omnetics connector, #A79012-001) to enable connecting it to the head stage before each experiment. Post-surgery, animals were administered daily injections of Norocarp (0.005 mg/gr) and Baytril (0.03 mL/10gr) for three days, allowing for a recovery period before engaging in experimental protocols. All animals were also implanted with electrodes, as previously described [38]. The results of the electrophysiological recordings will be published separately.

Head acceleration recording

Head acceleration was recorded in 3 axes (corresponding to surge, heave and sway, represented in Fig. 2A as X, Y, and Z axes, respectively) using an accelerometer (ADXL335, Analog Devices, Wilmington, MA) which was an integral part of the Intan electrophysiological recording

Table 2 Measures of the zero-g bias

Accelerometer			
Axis	**Mean voltage (V)**	**Sensitivity**	**Zero-g bias**
Z1	2,1086	0,3502	1,7584
Z2	1,4082		
Y1	2,0355	0,3387	1,6968
Y2	1,3581		
X1	2,0815	0,3494	1,7321
X2	1,3827		

head stage, with a range of 0.5 Hz to 1600 Hz for the X and Y axes and a range of 0.5 Hz to 550 Hz for the Z axis. We used two types of Intan head stages: 32 or 16 channels (Part #C3324 and Part #C3335, respectively, Intan Technologies, Los Angeles, CA). Before each session, the head stage was connected to the mice's skull using the abovementioned adapter, as illustrated in Fig. 1B. The acceleration recording was made with the Intan RHD2000 evaluation system using an ultra-thin SPI interface cable connected to the head stage through a manual commutator (Model # FL-89-OPT-12-C, Dragonfly, Inc., Ridgeley, WV). Acceleration recordings (sampled at 20 kHz and saved at 5 kHz) were synchronised with recorded video using a TTL trigger pulse and by recording camera frame strobes, as previously described [38].

Behavioural analysis

Subject behaviour was tracked using the TrackRodent software, designed for analysing the behaviour of wired mice, as previously described [66]. Notably, investigation bouts were automatically detected by the TrackRodent algorithm. Further analyses were conducted with the TrackRodent data using the DeepPhenotyping code written in MATLAB 2020a (see Table 3 below).

Extraction of head accelerometer data

The accelerometer reports both movement and the gravity vector. To calibrate the raw signal for each axis, we measured the voltage when the axis was aligned with the gravity vector in both directions. The zero-g bias for each axis was calculated as the average of these two measurements (e.g., Z1 and Z2 in Table 2 below). The sensitivity was determined by taking the voltage difference between these opposing positions and dividing it by 2. We then calibrated the raw signal by subtracting the corresponding zero-g bias for each axis (as shown in Table 2) and dividing the result by the corresponding sensitivity (Table 2), as described in the equation below.

For each axis:

$$Calibrated\ Accelaration = \left(Raw\ Acceleration - mean\ zero\ g\ bias\right)/meansensitivity$$

Table 3 Names of all code files used for each analysis (all codes may be found at: https://zenodo.org/records/14938315) [68]

	Matlab		Python
	File (.m)	**Function**	**File (.py)**
Figure 1 CDEF	Deephenotyping	GUI	Behavior
Figure 2	Plot_signal	SignalAcc_plot, DLC_signal_plot	
Figure 3 B-H	*Specific_Event*	SignalAcc, DLC_signal, Specific_Event_Beginning and Specific_Event_End	event_all
Figure 6			
Figure 7			
Figure 8			
Figure S2 B-E			
Figure 3 IJ	decoder	decoder_signal_z, SignalAcc, DLC_signal	decoder
Figure 4 AH	15min	Stage	15min
Figure S3			
Figure 4 IJ			sex_randomforest
Figure 5		Int	Interaction
Figure S4			
			All functions used are in function.py

From the calibrated accelerometer data, we extracted four components: Dynamic acceleration was obtained by applying a band-pass filter (1–100 Hz) to the calibrated acceleration data, separately for each axis (see Additional file 1: Fig. S1A). By applying a low-pass filter at 1 Hz to the calibrated acceleration data, we extracted the static component, which provides information about the inclination of the accelerometer relative to Earth's gravity, separately for each axis (see Additional file 1: Fig. S1B). The Arcsine function was applied to the X and Z axes of the static acceleration data to calculate the inclination angles as follows:

$$(X\ or\ Z)\_Asin\_Static = arcsin(Acceleration\ Static\ of\ X\ or\ Z)$$

Unlike the X and Z axes, the Y-axis is aligned with the gravity vector. Therefore, when the animal's head is flat, the accelerometer will register a value of 1 G. When the mouse tilts its head downward or upward, the accelerometer signal decreases towards 0 G. Because we wanted the values (angles in radians) of all axes to be 0 when the mouse head is in its flat position, the Arccos function was applied to the Y axis of the static acceleration data to calculate the inclination angle as follows:

$$(Y)\_Acos\_Static = arccos(Acceleration\ Static\ of\ Y)$$

We then calculated, separately for the static and dynamic components, the square root of the sum of squares for all three axes which we termed OSHA and ODHA for the static and dynamic components, respectively.

$$OSHA = \sqrt{X\_Asin\_Static^2 + Y\_Acos\_Static^2 + Z\_Asin\_Static^2}$$

$$ODHA = \sqrt{X\_Dynamic^2 + Y\_Dynamic^2 + Z\_Dynamic^2}$$

The ODHA reflects the energy of head movement, while the OSHA reflects the general tilt of the head from flat position (when OSHA equals zero).

To calculate the Roll, we considered the position of the accelerometer on the animal's head. When the animal's head is flat (parallel to the earth's surface) and stationary, the Z-axis of the accelerometer will return to a value of 0 G, as it is perpendicular to the gravity vector. To determine the extent of head rolling, regardless of direction, we took the absolute value of the static signal.

$$Roll = abs(Z\_Asin\_Static)$$

We calculated the Pitch using the low pass filtered Y-axis angle. As we mentioned already, the Y-axis is aligned with the gravity vector. Since the head of the animal is naturally never upside-down, the Y-axis is not expected to get a negative value. Therefore, it is not necessary to use the absolute value of this signal. Thus, we applied the following formula:

$$Pitch = Y\_cos\_Static$$

Video analysis with DeepLabCut (DLC)

DLC software (v.2.3.5, multi-animal DLC) [39] was used to track the positions of the subject body parts. The training set included 600 frames from three out of 277 sessions (male and female mice). The following head parts were marked in each frame: left ear, right ear, nose and neck. The model was trained by 2*106 iterations with default parameters (training frames selected by k-means clustering of each of the three videos, trained on 95% of labelled frames, initialised with dlcrnet_ms5, batch size of 8). When the likelihood for one or two frames was less than 0.90, we filled in the missing data by averaging the data from the frame before and the frame after. This smoothing technique helped ensure a consistent and reliable analysis dataset, particularly when the tracking accuracy was temporarily compromised. We used codes written in MATLAB 2020a to extract three parameters at different time windows and normalisation (Table 2): the average speed of these four parts of the head, the distance between the ears, and the distance between the nose and the neck. Additional file 2: Table 2 provides the percentage of frames with a likelihood above 0.90 for each session. Notably, when analysing DLC data over each of the three session stages (pre-test, test and post-test), extreme peaks were observed despite filtering for frames with likelihoods above 0.90. As shown in Fig. 2L, these peaks could reach 1,000 times the median, significantly skewing the mean values over one-minute or five-minute intervals. To mitigate this issue, we filtered the DLC data by removing values that exceeded three times the median (when Z-scoring wasn't applied).

Analysis of head acceleration or DLC data relative to investigation bouts

The data were extracted using MATLAB 2023a scripts, while all plots and statistical analyses were performed in Python using Spyder. Details of the code used for each figure are provided in Table 3. Only investigation bouts lasting longer than two seconds were considered for analysing data around investigation bouts. For event-specific analyses, we z-scored the signal across a four-second time window two seconds before and two seconds after each event (start or end of an investigation bout). The first second of this time window was used as a baseline. For data smoothing and removal of extreme values, z-score values were capped at thresholds of 1.9 and −1.9, representing

the significance cutoffs for positive and negative values, respectively.

Decision tree classifier model

In this study, we classified two types of labels (approaching vs. leaving, female vs. male). For each type of label, we trained a model using data extracted from either the accelerometer or DLC. To extract the various features, we implemented custom code in MATLAB 2024a.

The first classification focused on distinguishing between "approaching" and "leaving." Specifically, this involved identifying the second when the mouse approached or left the chamber. We extract each one of the parameters (summarised in Table 4) by applying a sliding mean across a half-second time window (using a 1-s bin). The accelerometer and DLC data were aligned with video annotations scored using TrackRodent (as previously described), and each 1-s bin was labelled with the most representative behaviour.

The second classification distinguished between the male and female, based on the 5-min test stage. We used data extracted during this period to train the model, as summarised in Table 5.

Both models were trained and tested using the *RandomForestClassifier* function from the Scikit-learn package in Python. We trained binary Random Forest classifiers to discriminate between the type of behavioural event or the mouse's sex. If necessary, we balanced the training set by randomly removing samples to ensure an equal number of samples from each class. The classifier was configured with 100 random trees (a parameter of the *RandomForestClassifier* function). We employed a cross-validation strategy where at least four mice (and 16 sessions) were left out during training for the testing set. We computed a confusion matrix based on the testing set.

To test whether the distribution of the confusion matrices was independent, we performed a Chi-square test of independence using the *chi2_contingency* function from the SciPy package in Python.

Statistical analysis

Statistical analysis and figure plotting were conducted using Spyder (version 5.4.1). Figures were generated using the Seaborn package (version 0.12.0 and 0.11.0), while statistical analyses were performed with the Pinguin package (version 0.5.4) [69]. Normality checks were performed using the Shapiro–Wilk test, homoscedasticity checks using the Levene test, and sphericity using the Mauchly test. Parametric tests were conducted when assumptions were met. Paired t-tests and independent t-tests were used to compare means between the two groups according to their dependence. Two-way ANOVA was employed for comparisons among multiple groups. For repeated measures, one-way repeated-measures ANOVA, or mixed-model ANOVA, were conducted according to the pattern of repetition. Non-parametric alternatives such as Wilcoxon, Mann–Whitney-Wilcoxon, Kruskal, and Friedman were used when assumptions were unmet. Post hoc

Table 4 Features for the decision tree 1 model

Approaching or Leaving (1s chunk)					
Acceleration			DLC		
OSHA	ODHA	Roll	Speed Head	Distance between ears	Distance nose to neck
Mean of the raw data for 1s chunck with running mean of 0.5s					
Standard deviation of the raw data for 1s chunck with running mean of 0.5s					
Min of the raw data for 1s chunck with running mean of 0.5s					
Max of the raw data for 1s chunck with running mean of 0.5s					
Mean of the Zscore data with the second before					
Standard deviation of the Zscore data with the second before					
Min of the Zscore data with the second before					
Max of the Zscore data with the second before					

Table 5 Feature for the decision tree 2

Female or male : for the all 5 minutes during the test					
Acceleration			DLC		
OSHA	ODHA	Roll	Speed Head	Distance between ears	Distance nose to neck
Mean for 5 min					
Standard deviation for 5 min					
Max for 5 min					
Min for 5 min					

analyses, following the observation of main effects, were carried out using False Discovery Rate Benjamini & Hochberg (FDR-BH) correction, implemented through the Statannotations package. All results and details of the statistical tests are summarised in Additional file 3.

Abbreviations

OSHA	Overall Static Head Acceleration
ODHA	Overall Dynamic Head Acceleration
SP	Social Preference
SxP	Sex Preference
ISP	Isolation State Preference
SSP	Social State Preference
DLC	Deep Lab Cut

Supplementary Information

The online version contains supplementary material available at https://doi.org/10.1186/s12915-025-02191-1.

Additional file 1: Figures S1-S5. FigS1 – [Separating the dynamic and static components of the accelerometer raw data]. Fig S2 - [Investigation time during the pre-test and test stages]. Fig S3 – [DLC analysis of the various head parts]. Fig S4 – [DLC-based changes in head kinematics along the session]. Fig S5 – [Differences in head acceleration variables during chamber investigation between pre-test (empty chambers) and test (stimulus-containing chambers) stages]

Additional file 2: Tables 1 and 2. Table 1: Summary of missing files. Table 2: DeepLabCut evaluation

Additional file 3: Details of all statistical analyses

Acknowledgements
We thank Eng. Alex Bizer, the experimental systems engineer of the Faculty of Natural Sciences of the University of Haifa, for his technical help.
Some parts of the figures have been created using BioRender.com.

Authors' contributions
A.P.: Formal analysis, Investigation, Methodology, Validation, Visualization, Writing—original draft, and Writing—review & editing; S.N.: Data curation, Project administration, Software, Validation, Visualization, Writing—original draft, and Writing—review & editing. S.W.: Conceptualization, Funding acquisition, Project administration, Resources, Supervision, Writing—original draft, and Writing—review & editing.

Funding
This study was supported by ISF-NSFC joint research program (grant No. 3459/20), the Israel Science Foundation (grants No. 1361/17 and 2220/22), the Ministry of Science, Technology and Space of Israel (Grant No. 3–12068), the Ministry of Health of Israel (grant #3–18380), the German Research Foundation (DFG) (GR 3619/16–1 and SH 752/2–1), the Congressionally Directed Medical Research Programs (CDMRP) (grant No. AR210005) and the United States-Israel Binational Science Foundation (grant No. 2019186).

Data availability
All data generated or analysed during this study are included in this published article, its supplementary information files and publicly available repositories (*Zenodo*: https://zenodo.org/records/14938315) [68].

Declarations

Ethics approval and consent to participate
All experimental procedures were approved by the Institutional Animal Care and Use Committee of the University of Haifa (UoH-IL2203-139, 1077U).

Consent of publication
All authors read and approved the final manuscript.

Competing interests
The authors declare that they have no competing interests.

Received: 25 April 2024 Accepted: 10 March 2025
Published online: 20 March 2025

References

1. Wiley RH. Specificity and multiplicity in the recognition of individuals: implications for the evolution of social behaviour. Biol Rev. 2013;88:179–95.
2. Langford DJ, Tuttle AH, Brown K, Deschenes S, Fischer DB, Mutso A, et al. Social approach to pain in laboratory mice. Soc Neurosci. 2010;5:163–70.
3. Kiyokawa Y, Honda A, Takeuchi Y, Mori Y. A familiar conspecific is more effective than an unfamiliar conspecific for social buffering of conditioned fear responses in male rats. Behav Brain Res. 2014;267:189–93.
4. Rogers-Carter MM, Djerdjaj A, Gribbons KB, Varela JA, Christianson JP. Insular Cortex Projections to Nucleus Accumbens Core Mediate Social Approach to Stressed Juvenile Rats. J Neurosci. 2019;39:8717–29.
5. Ferretti V, Papaleo F. Understanding others: Emotion recognition in humans and other animals. Genes Brain Behav. 2019;18: e12544.
6. Dunbar RIM. The social brain hypothesis and its implications for social evolution. Ann Hum Biol. 2009;36:562–72.
7. Jabarin R, Netser S, Wagner S. Beyond the three-chamber test: toward a multimodal and objective assessment of social behavior in rodents. Mol Autism. 2022;13:41.
8. Parker PRL, Brown MA, Smear MC, Niell CM. Movement-Related Signals in Sensory Areas: Roles in Natural Behavior. Trends Neurosci. 2020;43:581–95.
9. Niell CM, Stryker MP. Modulation of Visual Responses by Behavioral State in Mouse Visual Cortex. Neuron. 2010;65:472–9.
10. Saleem AB, Ayaz A, Jeffery KJ, Harris KD, Carandini M. Integration of visual motion and locomotion in mouse visual cortex. Nat Neurosci. 2013;16:1864–9.
11. Ayaz A, Saleem AB, Schölvinck ML, Carandini M. Locomotion controls spatial integration in mouse visual cortex. Curr Biol CB. 2013;23:890–4.
12. Meyer AF, Poort J, O'Keefe J, Sahani M, Linden JF. A Head-Mounted Camera System Integrates Detailed Behavioral Monitoring with Multichannel Electrophysiology in Freely Moving Mice. Neuron. 2018;100:46-60.e7.
13. Brown DD, Kays R, Wikelski M, Wilson R, Klimley AP. Observing the unwatchable through acceleration logging of animal behavior. Anim Biotelemetry. 2013;1:20.
14. Portugal SJ, Hubel TY, Fritz J, Heese S, Trobe D, Voelkl B, et al. Upwash exploitation and downwash avoidance by flap phasing in ibis formation flight. Nature. 2014;505:399–402.
15. Chimienti M, Cornulier T, Owen E, Bolton M, Davies IM, Travis JMJ, et al. The use of an unsupervised learning approach for characterizing latent behaviors in accelerometer data. Ecol Evol. 2016;6:727–41.
16. Collins PM, Green JA, Warwick-Evans V, Dodd S, Shaw PJA, Arnould JPY, et al. Interpreting behaviors from accelerometry: a method combining simplicity and objectivity. Ecol Evol. 2015;5:4642–54.
17. Shepard E, Wilson R, Quintana F, Gómez Laich A, Liebsch N, Albareda D, et al. Identification of animal movement patterns using tri-axial accelerometry. Endanger Species Res. 2008;10:47–60.
18. Nathan R, Spiegel O, Fortmann-Roe S, Harel R, Wikelski M, Getz WM. Using tri-axial acceleration data to identify behavioral modes of free-ranging animals: general concepts and tools illustrated for griffon vultures. J Exp Biol. 2012;215(Pt 6):986–96.
19. Sundararajan K, Georgievska S, te Lindert BHW, Gehrman PR, Ramautar J, Mazzotti DR, et al. Sleep classification from wrist-worn accelerometer data using random forests. Sci Rep. 2021;11:24.
20. Schalkamp A-K, Peall KJ, Harrison NA, Sandor C. Wearable movement-tracking data identify Parkinson's disease years before clinical diagnosis. Nat Med. 2023;29:2048–56.
21. Santos GL, Endo PT, Monteiro KH de C, Rocha E da S, Silva I, Lynn T. Accelerometer-Based Human Fall Detection Using Convolutional Neural Networks. Sensors. 2019;19:1644.

22. Pasquet MO, Tihy M, Gourgeon A, Pompili MN, Godsil BP, Léna C, et al. Wireless inertial measurement of head kinematics in freely-moving rats. Sci Rep. 2016;6:35689.
23. Shih Y-H, Young M-S. Integrated digital image and accelerometer measurements of rat locomotor and vibratory behaviour. J Neurosci Methods. 2007;166:81–8.
24. Mackrous I, Carriot J, Cullen KE. Context-independent encoding of passive and active self-motion in vestibular afferent fibers during locomotion in primates. Nat Commun. 2022;13:120.
25. Alves JA, Boerner BC, Laplagne DA. Flexible Coupling of Respiration and Vocalizations with Locomotion and Head Movements in the Freely Behaving Rat. Neural Plast. 2016;2016:1–16.
26. Sunderam S, Chernyy N, Peixoto N, Mason JP, Weinstein SL, Schiff SJ, et al. Improved Sleep-Wake and Behavior Discrimination Using MEMS Accelerometers. J Neurosci Methods. 2007;163:373–83.
27. Wilson R, Shepard E, Liebsch N. Prying into the intimate details of animal lives: Use of a daily diary on animals. Endanger Species Res. 2008;4:123–37.
28. Wilson RP, White CR, Quintana F, Halsey LG, Liebsch N, Martin GR, et al. Moving towards acceleration for estimates of activity-specific metabolic rate in free-living animals: the case of the cormorant. J Anim Ecol. 2006;75:1081–90.
29. Boisclair D, Leggett WC. The Importance of Activity in Bioenergetics Models Applied to Actively Foraging Fishes. Can J Fish Aquat Sci. 1989;46:1859–67.
30. Karasov WH, Anderson RA. Interhabitat Differences in Energy Acquisition and Expenditure in a Lizard. Ecology. 1984;65:235–47.
31. Tatner P, Bryant DM. Flight Cost of a Small Passerine Measured Using Doubly Labeled Water: Implications for Energetics Studies. Auk. 1986;103:169–80.
32. Meijer SW, Bramson B, Toni I, Roelofs K. Improving emotion control in social anxiety by tar-geting rhythmic brain activity. bioRxiv. 2024.
33. Halsey LG, Shepard ELC, Quintana F, Gomez Laich A, Green JA, Wilson RP. The relationship between oxygen consumption and body acceleration in a range of species. Comp Biochem Physiol A Mol Integr Physiol. 2009;152:197–202.
34. Halsey LG, Shepard ELC, Hulston CJ, Venables MC, White CR, Jeukendrup AE, et al. Acceleration versus heart rate for estimating energy expenditure and speed during locomotion in animals: Tests with an easy model species. Homo sapiens Zoology. 2008;111:231–41.
35. Halsey LG, Shepard ELC, Wilson RP. Assessing the development and application of the accelerometry technique for estimating energy expenditure. Comp Biochem Physiol A Mol Integr Physiol. 2011;158:305–14.
36. Kopachev N, Netser S, Wagner S. Sex-dependent features of social behavior differ between distinct laboratory mouse strains and their mixed offspring. iScience. 2022;25:103735.
37. Netser S, Haskal S, Magalnik H, Wagner S. A novel system for tracking social preference dynamics in mice reveals sex- and strain-specific characteristics. Mol Autism. 2017;8:53.
38. Mohapatra AN, Netser S, Wagner S. Modular Electrode Array for Multi-site Extracellular Recordings from Brains of Freely Moving Rodents. Curr Protoc. 2022;2:e399.
39. Multi-animal pose estimation, identification and tracking with DeepLabCut | Nature Methods. https://www.nature.com/articles/s41592-022-01443-0. Accessed 22 Mar 2024.
40. Shepard ELC, Wilson RP, Halsey LG, Quintana F, Gómez Laich A, Gleiss AC, et al. Derivation of body motion via appropriate smoothing of acceleration data. Aquat Biol. 2009;4:235–41.
41. Yoda K, Naito Y, Sato K, Takahashi A, Nishikawa J, Ropert-Coudert Y, et al. A new technique for monitoring the behaviour of free-ranging Adelie penguins. J Exp Biol. 2001;204:685–90.
42. Tendler A, Wagner S. Different types of theta rhythmicity are induced by social and fearful stimuli in a network associated with social memory. eLife. 2015;4:e03614.
43. Mohapatra AN, Peles D, Netser S, Wagner S. Synchronized LFP rhythmicity in the social brain reflects the context of social encounters. Commun Biol. 2024;7:1–18.
44. Benchenane K, Tiesinga PH, Battaglia FP. Oscillations in the prefrontal cortex: a gateway to memory and attention. Curr Opin Neurobiol. 2011;21:475–85.
45. Buzsáki G, Draguhn A. Neuronal oscillations in cortical networks. Science. 2004;304:1926–9.
46. Clayton MS, Yeung N, Cohen KR. The roles of cortical oscillations in sustained attention. Trends Cogn Sci. 2015;19:188–95.
47. Knyazev GG. Motivation, emotion, and their inhibitory control mirrored in brain oscillations. Neurosci Biobehav Rev. 2007;31:377–95.
48. Vinogradova OS. Expression, control, and probable functional significance of the neuronal theta-rhythm. Prog Neurobiol. 1995;45:523–83.
49. Wang X-J. Neurophysiological and computational principles of cortical rhythms in cognition. Physiol Rev. 2010;90:1195–268.
50. Karakaş S. A review of theta oscillation and its functional correlates. Int J Psychophysiol Off J Int Organ Psychophysiol. 2020;157:82–99.
51. Kleinfeld D, Deschênes M, Ulanovsky N. Whisking, Sniffing, and the Hippocampal θ-Rhythm: A Tale of Two Oscillators. PLoS Biol. 2016;14:e1002385.
52. Mauvais-Jarvis F. Sex differences in energy metabolism: natural selection, mechanisms and consequences. Nat Rev Nephrol. 2024;20:56–69.
53. Hammal Z, Cohn JF, George DT. Interpersonal Coordination of Head Motion in Distressed Couples. IEEE Trans Affect Comput. 2014;5:155–67.
54. Hammal Z, Cohn JF, Messinger DS. Head Movement Dynamics During Play and Perturbed Mother-Infant Interaction. IEEE Trans Affect Comput. 2015;6:361–70.
55. Boker SM, Cohn JF, Theobald B-J, Matthews I, Mangini M, Spies JR, et al. Something in the way we move: Motion dynamics, not perceived sex, influence head movements in conversation. J Exp Psychol Hum Percept Perform. 2011;37:874–91.
56. Ashenfelter KT, Boker SM, Waddell JR, Vitanov N. Spatiotemporal symmetry and multifractal structure of head movements during dyadic conversation. J Exp Psychol Hum Percept Perform. 2009;35:1072–91.
57. McDonald DQ, Zampella CJ, Sariyanidi E, Manakiwala A, DeJardin E, Herrington JD, et al. Head Movement Patterns during Face-to-Face Conversations Vary with Age. ICMI22 Companion Companion Publ 2022 Int Conf Multimodal Interact Novemb 7–11 2022 Bangalore India ICMI Conf 2022 Bangalore India. 2022;2022:185.
58. Fenollar-Cortés J, Gallego-Martínez A, Fuentes LJ. The role of inattention and hyperactivity/impulsivity in the fine motor coordination in children with ADHD. Res Dev Disabil. 2017;69:77–84.
59. Franchini M, Duku E, Armstrong V, Brian J, Bryson SE, Garon N, et al. Variability in Verbal and Nonverbal Communication in Infants at Risk for Autism Spectrum Disorder: Predictors and Outcomes. J Autism Dev Disord. 2018;48:3417–31.
60. Jahn T, Cohen R, Hubmann W, Mohr F, Köhler I, Schlenker R, et al. The Brief Motor Scale (BMS) for the assessment of motor soft signs in schizophrenic psychoses and other psychiatric disorders. Psychiatry Res. 2006;142:177–89.
61. American Psychiatric Association, editor. Diagnostic and statistical manual of mental disorders: DSM-IV ; includes ICD-9-CM codes effective 1. Oct. 96. 4. ed., 7. print. Washington, DC; 1998.
62. Fournier KA, Hass CJ, Naik SK, Lodha N, Cauraugh JH. Motor coordination in autism spectrum disorders: a synthesis and meta-analysis. J Autism Dev Disord. 2010;40:1227–40.
63. Quezada NT, Salas-Ortíz SF, Peralta FA, Aguayo FI, Morgado-Gallardo KP, Mac-Rae CA, et al. Loss of Social/Non-social Context Discrimination by Movement Acceleration in the Valproate Model of Autism. Front Behav Neurosci. 2020;14:555610.
64. Budman I, Meiri G, Ilan M, Faroy M, Langer A, Reboh D, et al. Quantifying the social symptoms of autism using motion capture. Sci Rep. 2019;9:7712.
65. Investigating Neural Correlates of Behavior in Freely Behaving Rodents Using Inertial Sensors. https://journals.physiology.org/doi/epdf/https://doi.org/10.1152/jn.00121.2010. Accessed 11 Sep 2024.
66. Netser S, Haskal S, Magalnik H, Bizer A, Wagner S. A System for Tracking the Dynam-ics of Social Preference Behavior in Small Rodents. J Vis Exp JoVE. 2019. https://doi.org/10.3791/60336.
67. Mohapatra AN, Jabarin R, Ray N, Netser S, Wagner S. Impaired emotion recognition in Cntnap2-deficient mice is associated with hyper-synchronous prefrontal cortex neuronal activity. 2023;:2023.10.19.563055.
68. Phalip A. Sex- and social context-dependent differences in mice head movement during social interactions. 2025. Zenodo. https://doi.org/10.5281/zenodo.14938315.
69. Vallat R. Pingouin: statistics in Python. J Open Source Softw. 2018;3:1026.

Publisher's Note